Arteriosclerosis, Thrombosis, and Vascular Biology

BASIC SCIENCES

ASGR1 Deficiency Inhibits Atherosclerosis in Western Diet–Fed *ApoE*$^{-/-}$ Mice by Regulating Lipoprotein Metabolism and Promoting Cholesterol Efflux

Yuyan Zhang,* Xinhai Jiang,* Weizhi Wang,* Lijuan Lei, Ren Sheng, Shunwang Li, Jinque Luo, Huan Liu, Jing Zhang, Xiaowan Han, Yining Li, Yuhao Zhang, Chenyin Wang, Shuyi Si, Zheng-Gen Jin, Yanni Xu

BACKGROUND: Atherosclerosis is the most common cause of cardiovascular diseases. Clinical studies indicate that loss-of-function ASGR1 (asialoglycoprotein receptor 1) is significantly associated with lower plasma cholesterol levels and reduces cardiovascular disease risk. However, the effect of ASGR1 on atherosclerosis remains incompletely understood; whether inhibition of ASGR1 causes liver injury remains controversial. Here, we comprehensively investigated the effects and the underlying molecular mechanisms of ASGR1 deficiency and overexpression on atherosclerosis and liver injury in mice.

METHODS: We engineered *Asgr1* knockout mice (*Asgr1*$^{-/-}$), *Asgr1* and *ApoE* double-knockout mice (*Asgr1*$^{-/-}$*ApoE*$^{-/-}$), and ASGR1-overexpressing mice on an *ApoE*$^{-/-}$ background and then fed them different diets to assess the role of ASGR1 in atherosclerosis and liver injury.

RESULTS: After being fed a Western diet for 12 weeks, *Asgr1*$^{-/-}$*ApoE*$^{-/-}$ mice exhibited significantly decreased atherosclerotic lesion areas in the aorta and aortic root sections, reduced plasma VLDL (very-low-density lipoprotein) cholesterol and LDL (low-density lipoprotein) cholesterol levels, decreased VLDL production, and increased fecal cholesterol contents. Conversely, ASGR1 overexpression in *ApoE*$^{-/-}$ mice increased atherosclerotic lesions in the aorta and aortic root sections, augmented plasma VLDL cholesterol and LDL cholesterol levels and VLDL production, and decreased fecal cholesterol contents. Mechanistically, ASGR1 deficiency reduced VLDL production by inhibiting the expression of MTTP (microsomal triglyceride transfer protein) and ANGPTL3 (angiopoietin-like protein 3)/ANGPTL8 (angiopoietin-like protein 8) but increasing LPL (lipoprotein lipase) activity, increased LDL uptake by increasing LDLR (LDL receptor) expression, and promoted cholesterol efflux through increasing expression of LXRα (liver X receptor-α), ABCA1 (ATP-binding cassette subfamily A member 1), ABCG5 (ATP-binding cassette subfamily G member 5), and CYP7A1 (cytochrome P450 family 7 subfamily A member 1). These underlying alterations were confirmed in ASGR1-overexpressing *ApoE*$^{-/-}$ mice. In addition, ASGR1 deficiency exacerbates liver injury in Western diet–induced *Asgr1*$^{-/-}$*ApoE*$^{-/-}$ mice and high-fat diet–induced but not normal laboratory diet–induced and high-fat and high-cholesterol diet–induced *Asgr1*$^{-/-}$ mice, while its overexpression mitigates liver injury in Western diet–induced ASGR1-overexpressing *ApoE*$^{-/-}$ mice.

CONCLUSIONS: Inhibition of ASGR1 inhibits atherosclerosis in Western diet–fed *ApoE*$^{-/-}$ mice, suggesting that inhibiting ASGR1 may serve as a novel therapeutic strategy to treat atherosclerosis and cardiovascular diseases.

GRAPHIC ABSTRACT: A graphic abstract is available for this article.

Key Words: asialoglycoprotein receptor 1 ■ atherosclerosis ■ cardiovascular diseases ■ cholesterol efflux ■ lipoprotein metabolism

Correspondence to: Shuyi Si, PhD, Chinese Academy of Medical Sciences & Peking Union Medical College, Beijing, China, Email sisyimb@hotmail.com; or Zheng-Gen Jin, PhD, University of Rochester School of Medicine and Dentistry, Rochester, NY, Email zheng-gen_jin@urmc.rochester.edu; or Yanni Xu, MD, Chinese Academy of Medical Sciences & Peking Union Medical College, Beijing, China, Email xuyanniwendeng@hotmail.com

*Y. Zhang, X. Jiang, and W. Wang contributed equally.

Supplemental Material is available at https://www.ahajournals.org/doi/suppl/10.1161/ATVBAHA.124.321076.

For Sources of Funding and Disclosures, see page 2447.

Arterioscler Thromb Vasc Biol is available at www.ahajournals.org/journal/atvb

Nonstandard Abbreviations and Acronyms

AAV	adeno-associated virus
ABCA1	ATP-binding cassette subfamily A member 1
ABCG5	ATP-binding cassette subfamily G member 5
ACC	acetyl-CoA carboxylase
ALT	alanine aminotransferase
AMPK	AMP-activated protein kinase
ANGPTL3	angiopoietin-like protein 3
ANGPTL4	angiopoietin-like protein 4
ANGPTL8	angiopoietin-like protein 8
ASGPR	asialoglycoprotein receptor
ASGR1	asialoglycoprotein receptor 1
AST	aspartate aminotransferase
CRISPR/Cas9	clustered regularly interspaced short palindromic repeats/clustered regularly interspaced short palindromic repeat–associated 9
CVD	cardiovascular disease
CYP7A1	cytochrome P450 family 7 subfamily A member 1
DEG	differentially expressed gene
FPLC	fast protein liquid chromatography
H&E	hematoxylin and eosin
HDL-C	high-density lipoprotein cholesterol
HFD	high-fat diet
HL	hepatic lipase
HMGCR	3-hydroxy-3-methylglutaryl coenzyme A reductase
IDL	intermediate-density lipoprotein
INSIG1	insulin-induced gene 1
LDL	low-density lipoprotein
LDL-C	low-density lipoprotein cholesterol
LDLR	low-density lipoprotein receptor
LPL	lipoprotein lipase
LXRα	liver X receptor-α
MTTP	microsomal triglyceride transfer protein
ND	normal laboratory diet
NF-κB	nuclear factor-κB
ORO	oil red O
PCR	polymerase chain reaction
SREBP	sterol regulatory element-binding protein
TC	total cholesterol
TG	triglyceride
VLDL	very-low-density lipoprotein
WD	Western diet

Highlights

- ASGR1 (asialoglycoprotein receptor 1) deficiency in Western diet–fed *ApoE*$^{-/-}$ mice leads to lower plasma VLDL (very-low-density lipoprotein) cholesterol and LDL (low-density lipoprotein) cholesterol levels, decreases VLDL production, increases fecal cholesterol contents, and thus inhibits atherosclerosis, while ASGR1 overexpression aggravates atherosclerosis.
- *Asgr1*$^{-/-}$*ApoE*$^{-/-}$ mice show decreased VLDL secretion via a decrease in the expression of MTTP (microsomal triglyceride transfer protein) and an increase in VLDL clearance by inhibiting ANGPTL3/8 (angiopoietin-like protein 3/8) expression and increasing LPL (lipoprotein lipase) activity, while ASGR1-overexpressing *ApoE*$^{-/-}$ mice have the opposite effects.
- *Asgr1*$^{-/-}$*ApoE*$^{-/-}$ mice show increased fecal cholesterol contents via an increase in the protein expression levels of cholesterol efflux–related proteins, including LXRα (liver X receptor-α), ABCA1 (ATP-binding cassette subfamily A member 1), ABCG5 (ATP-binding cassette subfamily G member 5), and CYP7A1 (cytochrome P450 family 7 subfamily A member 1), and these underlying alterations are also confirmed in ASGR1-overexpressing *ApoE*$^{-/-}$ mice.
- ASGR1 deficiency exacerbates liver injury in Western diet–induced *Asgr1*$^{-/-}$*ApoE*$^{-/-}$ mice and high-fat diet–induced *Asgr1*$^{-/-}$ mice, while its overexpression mitigates liver injury in Western diet–induced ASGR1-overexpressing *ApoE*$^{-/-}$ mice.
- Inhibiting ASGR1 may serve as a novel therapeutic strategy to treat atherosclerosis and related cardiovascular diseases.

Cardiovascular diseases (CVDs) are the leading cause of death worldwide.[1,2] CVDs are a group of disorders of the heart and blood vessels, including coronary heart disease, cerebrovascular disease, and peripheral arterial disease, that cause a significant global health burden.[2,3] Atherosclerosis is characterized by the accumulation of lipid deposits in the intima of arterial walls, and atherosclerotic CVD is the major contributor to CVDs.[2] Low-density lipoprotein cholesterol (LDL-C) is a recognized risk factor for CVDs, and the cumulative LDL-C burden for an artery remains a principal determinant of atherosclerosis initiation and progression.[2,4,5] Non–high-density lipoprotein cholesterol (HDL-C; non–HDL-C=total cholesterol [TC] concentration−HDL-C concentration) is the sum of cholesterol accumulated in all proatherogenic lipoproteins (LDL [low-density lipoprotein], VLDL [very-low-density lipoprotein], IDL [intermediate-density lipoprotein], lipoprotein [a], chylomicrons [CMs], and CM remnants), and it is thought to be

See accompanying editorial on page 2450

a better predictor of CVD risk than LDL-C.[2,6–8] Despite intensive statin treatment to lower serum LDL-C levels, patients with established CVDs are often left with residual risk.[9] Therefore, this underscores the need for novel effective lipid-lowering therapeutic strategies for atherosclerosis and its related CVDs.[9]

ASGPR (asialoglycoprotein receptor) is mainly expressed in the liver and is a highly conserved transmembrane heteromeric receptor consisting of 2 subunits ASGR1 (ASGPR1; H1) and ASGR2 (H2).[8–11] ASGPR mediates the uptake of galactose-terminating and N-acetylgalactosamine–terminating glycoproteins, thus playing a pivotal role in the homeostasis of circulating glycoproteins in the blood.[11–13] An important genetic study recently showed that ASGR1 loss of function (ASGR1del12 variant) is significantly associated with lower non–HDL-C levels and reduced coronary artery disease and coronary heart disease risks, suggesting that ASGR1 may contribute to the development and progression of atherosclerosis.[4,6,8] Xu et al[14] discovered that ASGR1 deficiency in mice reduced serum cholesterol and triglyceride (TG) contents via upregulating INSIG1 (insulin-induced gene 1) and inhibiting SREBP (sterol regulatory element-binding protein) activation. Wang et al[15] showed that *Asgr1*$^{-/-}$ mice fed a high-fat/high-cholesterol/bile salt diet for 4 to 6 weeks decreased lipid levels in the serum and liver and increased cholesterol efflux and the concentrations of biliary cholesterol and bile acids in the gallbladder by stabilizing LXRα (liver X receptor-α) and increasing the expression of target genes such as *ABCA1* (ATP-binding cassette subfamily A member 1), *ABCG5* (ATP-binding cassette subfamily G member 5), *ABCG8* (ATP-binding cassette subfamily G member 8), and *CYP7A1* (cytochrome P450 family 7 subfamily A member 1).[16–18] Knockdown of *Asgr1* in LDLR (LDL receptor)-deficient (*Ldlr*$^{-/-}$) mice by ASGR1 adeno-associated virus (AAV) shRNAs (short hairpin RNA) prevented artery plaque formation and lipid deposition in the liver induced by the high-fat/high-cholesterol/bile salt diet.[15] Xie et al[19] demonstrated that *Asgr1*$^{-/-}$ pigs fed an atherogenic diet for 6 months had lower non–HDL-C levels than control pigs, and this decrease was associated with downregulated HMGCR (3-hydroxy-3-methylglutaryl coenzyme A reductase) and upregulated hepatic LDLR expression. Though ASGR1 deficiency decreased liver TC contents, it had no effect on liver TG contents and led to mild-to-moderate liver injury in pigs.[19] However, Shi et al[20] showed that ASGR1 knockdown suppressed inflammatory macrophages in livers and decreased the inflammatory cytokine levels in mice, thus alleviating liver injury and improving survival in sepsis. A recent study showed that ASGR1 deficiency promoted while ASGR1 overexpression alleviated acetaminophen-induced acute and CCl_4 (carbon tetrachloride)-induced chronic liver injuries in male mice.[21] Taken together, ASGR1 has emerged as a new therapeutic target for lowering cholesterol and may be a potential target for therapeutic intervention in atherosclerosis.[22] However, the comprehensive effect of ASGR1 knockout or overexpression in mice on the development of atherosclerosis remains incompletely understood; whether inhibition of ASGR1 causes liver injury remains controversial and needs to be figured out.

In this study, we comprehensively investigated the effects and the underlying molecular mechanisms of ASGR1 deficiency and overexpression on atherosclerosis and liver injury in mice. We first generated double-knockout mice for *Asgr1* and *ApoE* deficiency (*Asgr1*$^{-/-}$*ApoE*$^{-/-}$) and ASGR1-overexpressing *ApoE*$^{-/-}$ mice and then investigated the potential role and mechanism of ASGR1 deficiency and overexpression in atherosclerosis upon Western diet (WD) feeding. Our results showed that ASGR1 deficiency significantly retarded the development of atherosclerosis, whereas ASGR1 overexpression aggravated the development of atherosclerosis in *ApoE*$^{-/-}$ mice. Mechanistically, knockdown of *Asgr1* led to a reduction in VLDL production by inhibiting the protein expression of MTTP (microsomal TG transfer protein), increased VLDL-TG clearance by inhibiting ANGPTL3 (angiopoietin-like protein 3) and ANGPTL8 (angiopoietin-like protein 8) expression and increasing LPL (lipoprotein lipase) activity, and increased fecal cholesterol content by upregulating the expression of cholesterol efflux–related proteins; ASGR1 overexpression in *ApoE*$^{-/-}$ mice had the opposite effect on VLDL production, degradation, and cholesterol efflux. Furthermore, ASGR1 deficiency exacerbated liver injury in WD-induced *Asgr1*$^{-/-}$*ApoE*$^{-/-}$ mice and high-fat diet (HFD)–induced but not affected normal laboratory diet (ND)–induced and high-fat and high-cholesterol diet–induced *Asgr1*$^{-/-}$ mice, while its overexpression mitigated liver injury in WD-induced ASGR1-overexpressing *ApoE*$^{-/-}$ mice. Taken together, our study demonstrates the critical role of ASGR1 in the pathogenesis of atherosclerosis and suggests that ASGR1 could be a target for novel therapeutic strategies to combat atherosclerosis-associated CVDs, but its effect on liver injury should be noted.

MATERIALS AND METHODS

The authors declare that the in vivo lesion–supporting data are available within the article (and its Supplemental Material). The other data that support the findings of this study are available from the corresponding author upon reasonable request.

Animals

All experimental procedures involving animals were approved by and strictly followed the requirements of the Institutional Laboratory Animal Care and Use Committee of the Institute of Medicinal Biotechnology, Chinese Academy of Medical Sciences & Peking Union Medical College (Beijing, China), and University of Rochester (Rochester, NY). The mice were housed in a specific-pathogen-free (SPF) barrier facility in 12-hour light/dark cycles at 25 °C with free access to food and water.

Asgr1 Knockout and *Asgr1*$^{-/-}$*ApoE*$^{-/-}$ Double-Knockout Mice Construction

ApoE$^{-/-}$ mice were purchased from Vital River Laboratory Animal Technology Co., Ltd (Beijing, China). *Asgr1*$^{+/-}$ mice were generated by CRISPR/Cas9 (clustered regularly interspaced short palindromic repeats/clustered regularly interspaced short palindromic repeat–associated 9)-mediated genome engineering by Cyagen Bioscience, Inc (Guangzhou, China). *Asgr1*$^{-/-}$ mice were obtained by crossing female *Asgr1*$^{+/-}$ mice with male *Asgr1*$^{+/-}$ mice. *Asgr1*$^{+/-}$*ApoE*$^{-/-}$ mice were obtained by crossing *Asgr1*$^{-/-}$ mice with *ApoE*$^{-/-}$ mice. *Asgr1*$^{-/-}$*ApoE*$^{-/-}$ double-knockout mice were obtained by crossing female *Asgr1*$^{+/-}$*ApoE*$^{-/-}$ mice with male *Asgr1*$^{+/-}$*ApoE*$^{-/-}$ mice. The genotypes were determined by polymerase chain reaction (PCR) using DNA from the mouse ear. The primers used are shown in Table S1. The bands for *Asgr1* and *ApoE* were as follows: 659 bp (*Asgr1*$^{+/+}$), 896 bp (*Asgr1*$^{-/-}$), 659 and 896 bp (*Asgr1*$^{+/-}$), and 245 bp (*ApoE*$^{-/-}$).

WD-Induced ASGR1 Deficiency Atherosclerosis Model Construction

WD (No. TP26300, 21% fat, 0.2% cholesterol, 49.1% carbohydrate, and 19.8% protein % based on weight) was purchased from Trophic Animal Feed High-Tech Co., Ltd (Nantong, China). Eight-week-old male and female *Asgr1*$^{+/+}$*ApoE*$^{-/-}$, *Asgr1*$^{+/-}$*ApoE*$^{-/-}$, and *Asgr1*$^{-/-}$*ApoE*$^{-/-}$ littermate mice were fed WD feed for 12 weeks for atherosclerosis studies.

AAV8-ASGR1 Virus Preparation and ASGR1 Overexpression Atherosclerosis Model Construction

Briefly, pAAV-CMV (cytomegalovirus)>mAsgr1/HA (hemagglutinin)/T2A (Thosea asigna virus 2A)/EGFP (enhanced green fluorescent protein) plasmid containing mouse Asgr1 (NM_009714.3) sequences was constructed by Cyagen Bioscience (Guangzhou, China). The AAV8-ASGR1 adenoviral-associated viral vector (AAV-ASGR1) and control viral vector (AAV-Con) were then constructed by Cyagen Bioscience. α-Mouse liver 12 (AML12) cells purchased from ATCC (American type culture collection) were cultured in DMEM (Thermo Fisher Biochemical Products, Beijing, China), supplemented with 10% (v/v) fetal bovine serum (Gibco, NY) at 37 °C and 5% CO_2. AML12 cells were transfected with AAV-ASGR1 or AAV-Con for 48 hours, and then the total proteins were collected to analyze the protein expression of ASGR1 by Western blotting. Male and female *ApoE*$^{-/-}$ mice were randomly divided into *ApoE*$^{-/-}$+AAV-Con and *ApoE*$^{-/-}$+AAV-ASGR1 groups (12 mice per group). Mice were given tail vein injections of 1×10^{11} GC (genomic copies) AAV8-Con or AAV8-ASGR1, and then the mice were fed a WD (TP26300) for 12 weeks.

Tissue Processing

At the end of the experiments, mice were anesthetized with isoflurane and euthanized with regard for alleviation of suffering. Blood was collected from the orbital venous plexus, and then the mice were perfused with saline. Plasma was obtained from heparin-anticoagulated blood centrifuged for 15 minutes at 3000 rpm and stored at −80 °C. Some liver tissues, intestine, lung, kidney, and spleen were snap-frozen in liquid nitrogen and stored at −80 °C for further analysis. The aortas, hearts, and some livers were fixed in 4% paraformaldehyde and used for subsequent analyses.

Serum Lipids and Biochemical Measurements

Mice were fasted for 12 hours before being euthanized. Plasma TG, TC, LDL-C, glucose, ALT (alanine aminotransferase), and AST (aspartate aminotransferase) were measured using commercial kits (BioSino, Beijing, China) and an automatic blood biochemical analyzer (Hitachi 71800, Chiyoda, Japan). LPL activity in plasma was determined using a commercial kit (BC2445; Solarbio Life Sciences, Beijing, China) using a microplate reader (EnVision; PerkinElmer, Fremont, CA).

Fast Protein Liquid Chromatography Analysis

Complete details of this technique have been described previously.[23] The same volume of serum from each mouse of each group was pooled together. Then plasma (200 μL) of each group was separated by fast protein liquid chromatography (FPLC; see Supplemental Materials and Methods for a detailed protocol). Cholesterol contents in each FPLC fraction were determined.[23] The protein expression of ApoB in each FPLC fraction was analyzed by Western blotting.

Liver Lipid Measurement

Liver tissues were weighed and homogenized in 1 mL RIPA Lysis Buffer (APPLGEN, Beijing, China) using the GeneReady BSH-C2 UltraCoo1 system (Hangzhou LifeReal Biotechnology Co., Ltd, Hangzhou, China). Protein concentrations were quantified by a bicinchoninic acid assay protein assay kit (Thermo Fisher, Waltham, MA) according to the manufacturer's instructions. TC and TG contents in the liver were quantified using commercial kits (Applygen Technologies, Inc, Beijing, China) and then normalized for protein concentration (mmol/g protein or mmol/g liver tissue).

Histological Staining

The aortic sinus cryosections were stained with hematoxylin and eosin (H&E) using a commercial kit (Beyotime Biotechnology, Beijing, China) or oil red O (ORO) solution (MeilunBio, Liaoning, China). Images were acquired using the DM2500 orthomorphic microscope (Leica Microsystems). The average from 6 aortic sinus sections spanning ≈150 μm from each mouse was used to determine the lesion size. H&E staining and sirius red staining for liver paraffin sections were performed by Wuhan Servicebio Technology Co., Ltd. Images were acquired using a slide scanner (PANNORAMIC MIDI; 3DHISTECH, Ltd, Budapest, Hungary). H&E-stained mouse liver sections were scored according to the nonalcoholic fatty liver disease activity score rule under double-blinded conditions. Nonalcoholic fatty liver disease activity score is the sum of scores of steatosis (0–3), lobular inflammation (0–3), and ballooning (0–2).[24] Sirius red staining positive area percentage was calculated by ImageJ (National Institutes of Health). Please see the Supplemental Materials and Methods for the detailed experimental protocol.

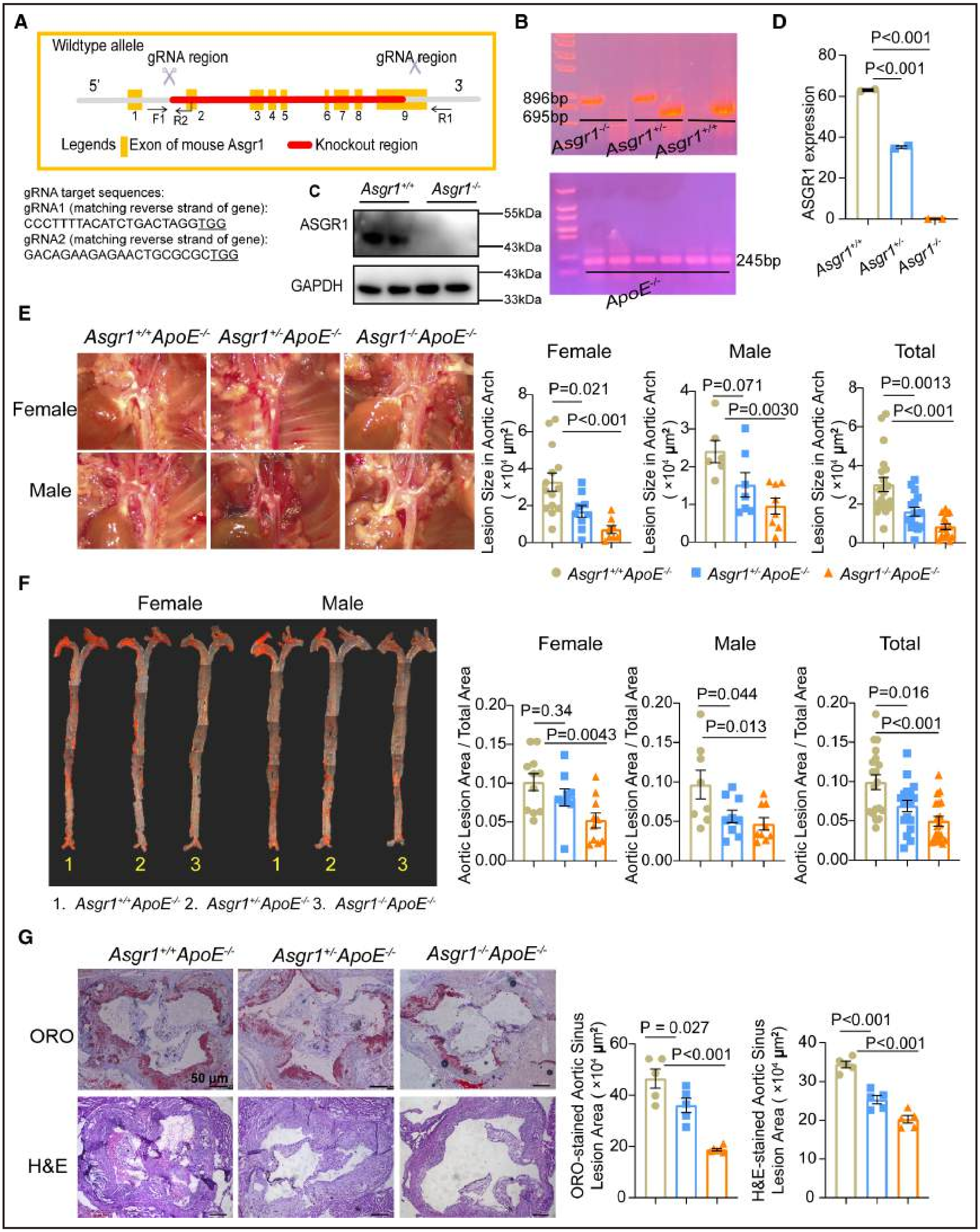

Figure 1. ASGR1 (asialoglycoprotein receptor 1) deficiency ameliorates Western diet (WD)–induced atherosclerosis in *ApoE*$^{-/-}$ mice.

A, Schematic showing the generation of *Asgr1*$^{-/-}$ mice. **B**, Distinct 659-bp (*Asgr1*$^{+/+}$), 896-bp (*Asgr1*$^{-/-}$), 659- and 896-bp (*Asgr1*$^{+/-}$), and 245-bp (*ApoE*$^{-/-}$) bands were observed by agarose gel electrophoresis after polymerase chain reaction (PCR) using DNA from ears. **C**, ASGR1 protein expression levels in livers from 8-week-old male *Asgr1*$^{+/+}$*ApoE*$^{-/-}$ and *Asgr1*$^{-/-}$*ApoE*$^{-/-}$ mice were analyzed by Western blotting. **D**, RNA-sequencing (RNA-seq) data of *Asgr1* expression in 8-week-old male *Asgr1*$^{+/+}$, *Asgr1*$^{+/-}$, and *Asgr1*$^{-/-}$ mice. **E** through **G**, (*Continued*)

Atherosclerosis Analysis

Images of the aortic arch were captured with the EZ4W stereomicroscope (Leica Microsystems). For the lesion area analysis of the en face aortas, the whole aortas were split and stained with ORO. The 4 to 6 images of each full-length aorta were captured using the S8APO microscope (Leica Microsystems) and then reassembled back to a whole aorta using the Word processing software. And the ratio of the atherosclerotic lesion area to the total aortic area (plaque/total) was assessed using the ImageJ software. To analyze the atherosclerotic lesion areas at the aortic sinus intersection, ORO and H&E were used to stain the heart cryosections.[25] The images were captured and analyzed using the DM2500 microscope (Leica Microsystems), and the atherosclerotic lesion areas were measured using the ImageJ software.

VLDL-TG Secretion Assay

Eight-week-old *Asgr1*$^{+/+}$, *Asgr1*$^{+/-}$, and *Asgr1*$^{-/-}$ mice were fed an ND. Eight-week-old *Asgr1*$^{+/+}$*ApoE*$^{-/-}$, *Asgr1*$^{+/-}$*ApoE*$^{-/-}$, *Asgr1*$^{-/-}$*ApoE*$^{-/-}$, *ApoE*$^{-/-}$+AAV-Con, and *ApoE*$^{-/-}$+AAV-ASGR1 mice were fed a WD for 12 weeks. To measure in vivo VLDL secretion in mice, the above mice were fasted for 12 hours and then injected with the lipase inhibitor tyloxapol (500 mg/kg IV; MedChemExpress, Shanghai, China) through the tail vein to block VLDL catabolism. Blood (50–80 µL) was collected from the retro-orbital plexus in heparinized tubes at 1, 2, and 3 hours. Plasma TC and TG levels were measured and the VLDL-TG production rate was calculated from the slope of the plasma TG versus time curve.[26]

RNA Sequencing and Bioinformatics Analysis

Fresh liver samples from 8-week-old male *Asgr1*$^{+/+}$, *Asgr1*$^{+/-}$, and *Asgr1*$^{-/-}$ mice were snap-frozen in liquid nitrogen and stored at −80 °C for use. RNA-sequencing analysis was performed by OE Biotech Co., Ltd (Shanghai, China). The genes expressed in *Asgr1*$^{+/-}$ and *Asgr1*$^{-/-}$ mice were compared with those in the *Asgr1*$^{+/+}$ group, and the fold changes were reported. More than 2-fold changes and a *P* value of <0.05 in comparison with the *Asgr1*$^{+/+}$ group were defined as differentially expressed genes (DEGs). DEGs were then analyzed based on gene ontology enrichment analysis, and key gene ontology terms were extracted.

Western Blotting

Antibodies used for Western blotting are listed in the Major Resources Table in the Supplemental Material. The ImageJ software was used to determine the protein amounts, and all target proteins were normalized to the loading control (GAPDH or β-tubulin). Please see the Supplemental Materials and Methods for the detailed experimental protocol.

RNA Isolation and Quantitative Real-Time PCR Assay

Total RNA from mouse livers and treated human hepatoma HepG2 cells were extracted. The mRNA expression levels of the genes were adjusted to those of the endogenous GAPDH control by quantitative real-time PCR (qRT-PCR) assay. The sequences of the primers are shown in Table S2. Please see Supplemental Materials and Methods for the detailed experimental protocol.

Statistical Analysis

All data are expressed as mean±SEM and were analyzed with the GraphPad Prism 8 software. A 2-tailed Student *t* test was used to compare the significance between 2 groups. One- or 2-way ANOVA was used when comparing ≥3 groups followed by the Dunnett post hoc test. $P<0.05$ was considered statistically significant.

RESULTS

ASGR1 Deficiency Attenuates the Development of Atherosclerosis in WD-Fed *ApoE*$^{-/-}$ Mice

To examine the role of ASGR1 in the development of atherosclerosis, we first generated *Asgr1* knockout mice (Figure 1A) and *Asgr1* and *ApoE* double-knockout mice. The genotypes of *Asgr1*$^{+/+}$, *Asgr1*$^{+/-}$, *Asgr1*$^{-/-}$, and *ApoE*$^{-/-}$ mice were identified by PCR (Figure 1B). Western blotting and RNA sequencing demonstrated that *Asgr1* was successfully deleted at the protein and mRNA level in both *Asgr1*$^{+/-}$ and *Asgr1*$^{-/-}$ mice compared with wild-type *Asgr1*$^{+/+}$ littermate controls at 8 weeks of age (Figure 1C and 1D). We then explored the effect of ASGR1 deficiency on atherosclerosis plaque development in *Asgr1*$^{+/-}$*ApoE*$^{-/-}$ and *Asgr1*$^{-/-}$*ApoE*$^{-/-}$ mice and littermate controls (*Asgr1*$^{+/+}$*ApoE*$^{-/-}$) fed a WD for 12 weeks.

Compared with *Asgr1*$^{+/+}$*ApoE*$^{-/-}$ mice, *Asgr1*$^{+/-}$*ApoE*$^{-/-}$ mice exhibited a decrease in lesions located at the aortic arch (48.69% in females, $P=0.021$; 37.00% in males, $P=0.071$; and 46.66% in total mice; $P=0.0013$; Figure 1E), and *Asgr1*$^{-/-}$*ApoE*$^{-/-}$ mice exhibited a significant decrease (78.53% in females, $P<0.001$, 60.30% in males, $P=0.0030$, and 72.51% in total mice, $P<0.001$) in lesions located at the aortic arch in both sexes (Figure 1E). Analysis of atherosclerotic lesion formation by ORO staining in whole en face aortas revealed a decrease in the lesion area in *Asgr1*$^{+/-}$*ApoE*$^{-/-}$ mice

Figure 1 Continued. Eight-week-old *Asgr1*$^{+/+}$*ApoE*$^{-/-}$, *Asgr1*$^{+/-}$*ApoE*$^{-/-}$, and *Asgr1*$^{-/-}$*ApoE*$^{-/-}$ mice were fed a WD for 12 weeks. **E**, Representative images and quantification of aortic arches are shown. Female *Asgr1*$^{+/+}$*ApoE*$^{-/-}$, n=14; female *Asgr1*$^{+/-}$*ApoE*$^{-/-}$, n=9; female *Asgr1*$^{-/-}$*ApoE*$^{-/-}$, n=8. Male *Asgr1*$^{+/+}$*ApoE*$^{-/-}$, n=6; male *Asgr1*$^{+/-}$*ApoE*$^{-/-}$, n=7; male *Asgr1*$^{-/-}$*ApoE*$^{-/-}$, n=8. Total *Asgr1*$^{+/+}$*ApoE*$^{-/-}$, n=20; total *Asgr1*$^{+/-}$*ApoE*$^{-/-}$, n=16; total *Asgr1*$^{-/-}$*ApoE*$^{-/-}$, n=16. **F**, Representative images and quantification of oil red O (ORO)–stained en face aortas are shown. Female *Asgr1*$^{+/+}$*ApoE*$^{-/-}$, n=11; female *Asgr1*$^{+/-}$*ApoE*$^{-/-}$, n=9; female *Asgr1*$^{-/-}$*ApoE*$^{-/-}$, n=10. Male *Asgr1*$^{+/+}$*ApoE*$^{-/-}$, n=8; male *Asgr1*$^{+/-}$*ApoE*$^{-/-}$, n=9; male *Asgr1*$^{-/-}$*ApoE*$^{-/-}$, n=9. Total *Asgr1*$^{+/+}$*ApoE*$^{-/-}$, n=19; total *Asgr1*$^{+/-}$*ApoE*$^{-/-}$, n=18; total *Asgr1*$^{-/-}$*ApoE*$^{-/-}$, n=19. **G**, Representative images and quantification of hematoxylin and eosin (H&E) or ORO staining of aortic sinus cross sections are shown. ORO staining, n=5 or 6 for each group; H&E staining, n=5 for each group. Bar lengths, 50 µm. Data were expressed as mean±SEM. Significant differences were determined by 1-way ANOVA compared with *Asgr1*$^{+/+}$*ApoE*$^{-/-}$ mice (**E** through **G**) or *Asgr1*$^{+/+}$ mice (**D**).

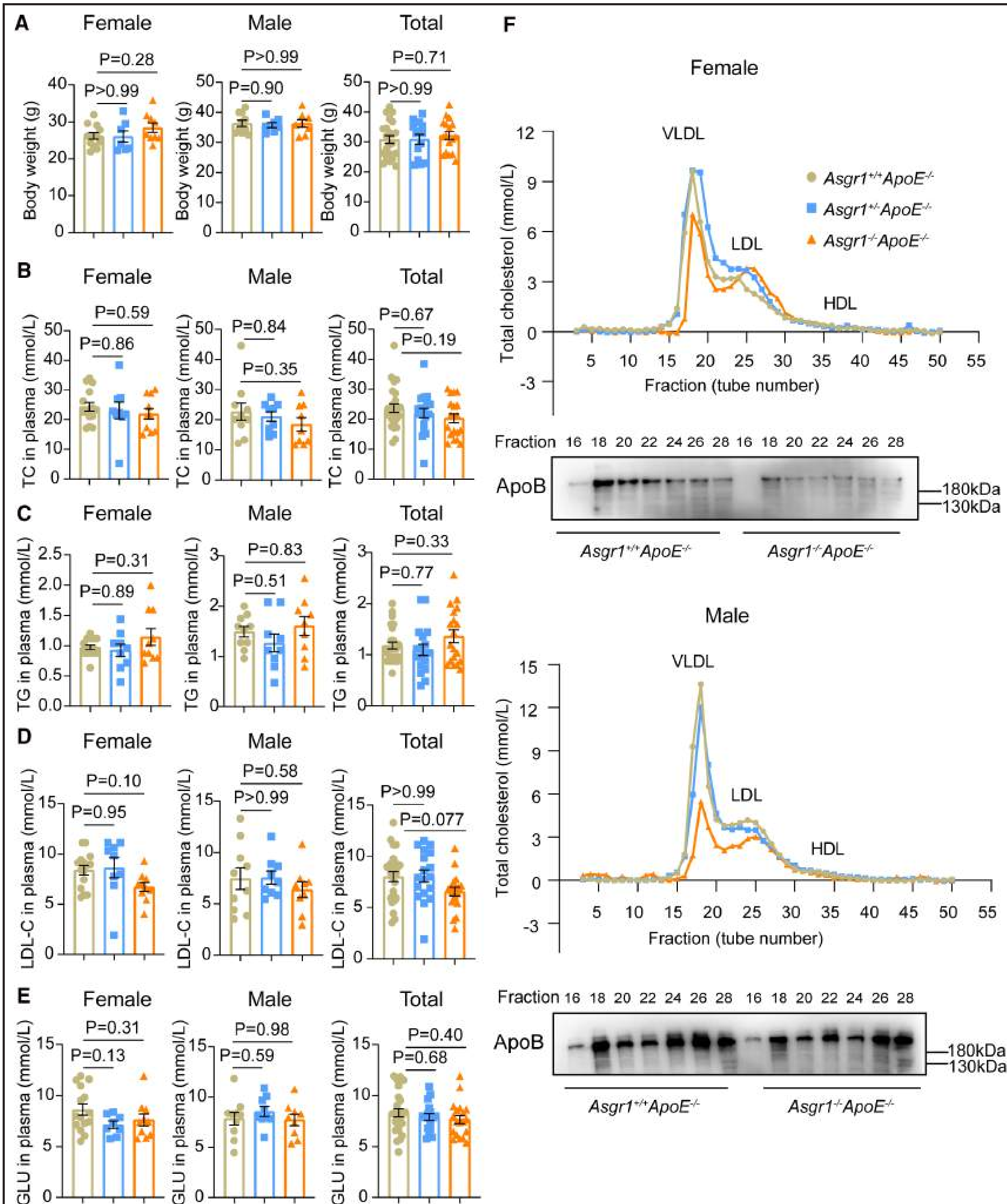

Figure 2. Effects of ASGR1 (asialoglycoprotein receptor 1) deficiency on plasma lipid profiles in *ApoE*$^{-/-}$ mice fed a Western diet (WD).

A through **E**, Body weight (**A**), total cholesterol (TC; **B**), triglyceride (TG; **C**), low-density lipoprotein cholesterol (LDL-C; **D**), and glucose (GLU; **E**) levels in plasma of 8-week-old $Asgr1^{+/+}ApoE^{-/-}$, $Asgr1^{+/-}ApoE^{-/-}$, and $Asgr1^{-/-}ApoE^{-/-}$ mice fed a WD for 12 weeks. **A**, Female $Asgr1^{+/+}ApoE^{-/-}$, n=12; female $Asgr1^{+/-}ApoE^{-/-}$, n=7; female $Asgr1^{-/-}ApoE^{-/-}$, n=9. Male $Asgr1^{+/+}ApoE^{-/-}$, n=10; male $Asgr1^{+/-}ApoE^{-/-}$, n=7; male $Asgr1^{-/-}ApoE^{-/-}$, n=8. Total $Asgr1^{+/+}ApoE^{-/-}$, n=22; total $Asgr1^{+/-}ApoE^{-/-}$, n=14; total $Asgr1^{-/-}ApoE^{-/-}$, n=17. **B** through **E**, Female $Asgr1^{+/+}ApoE^{-/-}$, n=15; female $Asgr1^{+/-}ApoE^{-/-}$, n=8 or 9; female $Asgr1^{-/-}ApoE^{-/-}$, n=10. Male $Asgr1^{+/+}ApoE^{-/-}$, n=10; male $Asgr1^{+/-}ApoE^{-/-}$, n=9; male $Asgr1^{-/-}ApoE^{-/-}$, n=9. Total $Asgr1^{+/+}ApoE^{-/-}$, n=25; total $Asgr1^{+/-}ApoE^{-/-}$, n=17 or 18; total $Asgr1^{-/-}ApoE^{-/-}$, n=19. **F**, Plasma cholesterol distribution and ApoB protein expression. Plasma was pooled from each group (n=7–9), and the distribution of plasma (*Continued*)

(19.23% in females, P=0.34; 41.62% in males, P=0.044; and 30.42% in total mice, P=0.016) and *Asgr1*$^{-/-}$*ApoE*$^{-/-}$ mice (48.46% in females, P=0.0043; 51.39% in males, P=0.013; and 49.93% in total mice, P<0.001) compared with female, male, and total *Asgr1*$^{+/+}$*ApoE*$^{-/-}$ mice, respectively (Figure 1F). All ORO-stained en face aorta images are shown in Figure S1.

In addition, ORO staining of aortic root sections showed smaller atherosclerotic plaque areas in *Asgr1*$^{+/-}$*ApoE*$^{-/-}$ mice (36.07±2.86×10^4 μm^2; P=0.027) and *Asgr1*$^{-/-}$*ApoE*$^{-/-}$ mice (18.83±0.49×10^4 μm^2; P<0.001) compared with *Asgr1*$^{+/+}$*ApoE*$^{-/-}$ mice (46.55±3.75×10^4 μm^2; Figure 1G). Similarly, H&E staining of aortic root sections also showed smaller atherosclerotic plaque areas in *Asgr1*$^{+/-}$*ApoE*$^{-/-}$ mice (25.30±1.07×10^4 μm^2; P<0.001) and *Asgr1*$^{-/-}$*ApoE*$^{-/-}$ mice (20.22±0.97×10^4 μm^2; P<0.001) compared with *Asgr1*$^{+/+}$*ApoE*$^{-/-}$ mice (34.38±0.83×10^4 μm^2; Figure 1G). All ORO- and H&E-stained aortic sinus cryosections are shown in Figure S2.

Collectively, these data demonstrate that ASGR1 deficiency alleviates atherosclerotic lesions in both male and female *Asgr1*$^{-/-}$*ApoE*$^{-/-}$ mice, and there were no significant differences between female and male mice.

ASGR1 Deficiency Decreases VLDL-C and LDL-C Levels in WD-Fed *ApoE*$^{-/-}$ Mice

The mean body weight of *Asgr1*$^{+/+}$*ApoE*$^{-/-}$, *Asgr1*$^{+/-}$*ApoE*$^{-/-}$, and *Asgr1*$^{-/-}$*ApoE*$^{-/-}$ mice was 30.80, 30.90, and 32.15 g, respectively, indicating that the depletion of ASGR1 did not affect body weight (Figure 2A). We then measured the plasma lipid levels, which are strongly related to atherosclerosis. *Asgr1*$^{+/-}$*ApoE*$^{-/-}$ and *Asgr1*$^{-/-}$*ApoE*$^{-/-}$ mice exhibited no significant changes in plasma TC and TG levels when compared with those in *Asgr1*$^{+/+}$*ApoE*$^{-/-}$ mice (Figure 2B and 2C). Plasma LDL-C levels were slightly decreased in *Asgr1*$^{-/-}$*ApoE*$^{-/-}$ mice but with no significant difference (P=0.10 for female mice, P=0.58 for male mice, and P=0.077 for total mice) compared with female, male, and total *Asgr1*$^{+/+}$*ApoE*$^{-/-}$ mice, respectively (Figure 2D). In addition, there were no obvious changes in plasma glucose levels in *Asgr1*$^{+/-}$*ApoE*$^{-/-}$ and *Asgr1*$^{-/-}$*ApoE*$^{-/-}$ mice compared with *Asgr1*$^{+/+}$*ApoE*$^{-/-}$ mice in both sexes (Figure 2E).

The lipoprotein profile of the pooled plasma of each group was tested by FPLC. The VLDL-C levels in female and male *Asgr1*$^{-/-}$*ApoE*$^{-/-}$ mice and LDL-C levels in male *Asgr1*$^{-/-}$*ApoE*$^{-/-}$ mice were lower than those in female and male *Asgr1*$^{+/+}$*ApoE*$^{-/-}$ mice, respectively (Figure 2F). Consistent with the lipoprotein results, the protein levels of ApoB were decreased in plasma fractions 16 to 20, which correspond to VLDL lipoproteins, in both female and male *Asgr1*$^{-/-}$*ApoE*$^{-/-}$ mice compared with *Asgr1*$^{+/+}$*ApoE*$^{-/-}$ mice (Figure 2F).

ASGR1 Deficiency Causes Liver Injury in WD-Fed *Asgr1*$^{-/-}$*ApoE*$^{-/-}$ Mice

Previous studies of whether ASGR1 deficiency causes liver damage have been controversial.[15,19] We measured liver lipid contents and the indices of liver function in *Asgr1* and *ApoE* double-knockout mice.

As shown in Figure 3A, TC contents in the liver were not different among the groups of either sex. The TG contents in the livers of female *Asgr1*$^{+/-}$*ApoE*$^{-/-}$ and *Asgr1*$^{-/-}$*ApoE*$^{-/-}$ mice were significantly decreased compared with female *Asgr1*$^{+/+}$*ApoE*$^{-/-}$ mice, but there were no changes in the TG contents in the livers of male mice and total mice (P=0.053 for total *Asgr1*$^{-/-}$*ApoE*$^{-/-}$ mice versus *Asgr1*$^{+/+}$*ApoE*$^{-/-}$ mice; Figure 3B). ORO staining results of liver sections showed that *Asgr1*$^{+/-}$*ApoE*$^{-/-}$ mice in both sexes and female *Asgr1*$^{-/-}$*ApoE*$^{-/-}$ mice had less lipid accumulation than that of *Asgr1*$^{+/+}$*ApoE*$^{-/-}$ mice (Figure 3C), while male *Asgr1*$^{-/-}$*ApoE*$^{-/-}$ mice had similar lipid accumulation with that of male *Asgr1*$^{+/+}$*ApoE*$^{-/-}$ mice (Figure 3C).

We next examined the plasma ALT and AST levels, which are the most widely used indicators of liver injury. The plasma ALT (P=0.16 for female mice, P=0.16 for male mice, and P=0.056 for total mice; Figure 3D) and AST (P=0.043 for female mice, P=0.44 for male mice, and P=0.050 for total mice; Figure 3E) increased in *Asgr1*$^{-/-}$*ApoE*$^{-/-}$ mice compared with the *Asgr1*$^{+/+}$*ApoE*$^{-/-}$ mice (Figure 3E). There were no significant differences in plasma ALT and AST levels between *Asgr1*$^{+/-}$*ApoE*$^{-/-}$ and *Asgr1*$^{+/+}$*ApoE*$^{-/-}$ mice in both sexes (Figure 3D and 3E). H&E staining and sirius red staining results of the liver sections showed that *Asgr1*$^{-/-}$*ApoE*$^{-/-}$ mice had significant worse liver morphology (Figure 3F and 3G) and more severe liver fibrosis (Figure 3H and 3I) than those of *Asgr1*$^{+/+}$*ApoE*$^{-/-}$ mice in both sexes, while *Asgr1*$^{+/-}$*ApoE*$^{-/-}$ mice had no obvious effects (Figure 3F through 3I). TUNEL (terminal deoxynucleotidyl transferase [TdT] dUTP nick-end labeling) staining results showed that ASGR1 deficiency had no obvious effects on hepatocyte apoptosis (Figure S3).

What is more, the plasma ALT and AST levels in HFD-fed *Asgr1*$^{+/-}$ mice, the plasma AST levels in HFD-fed *Asgr1*$^{-/-}$ mice, and sirius red staining results in HFD-fed *Asgr1*$^{-/-}$ mice were significantly increased compared with

Figure 2 Continued. cholesterol in different types of lipoproteins was determined after separation by fast protein liquid chromatography (FPLC). Protein expression levels of ApoB in the fractions of female and male *Asgr1*$^{+/+}$*ApoE*$^{-/-}$ and *Asgr1*$^{-/-}$*ApoE*$^{-/-}$ mice were analyzed by Western blotting. Data were statistically analyzed by 1-way ANOVA, and the values are expressed as mean±SEM. P values were calculated by comparison with the *Asgr1*$^{+/+}$*ApoE*$^{-/-}$ group.

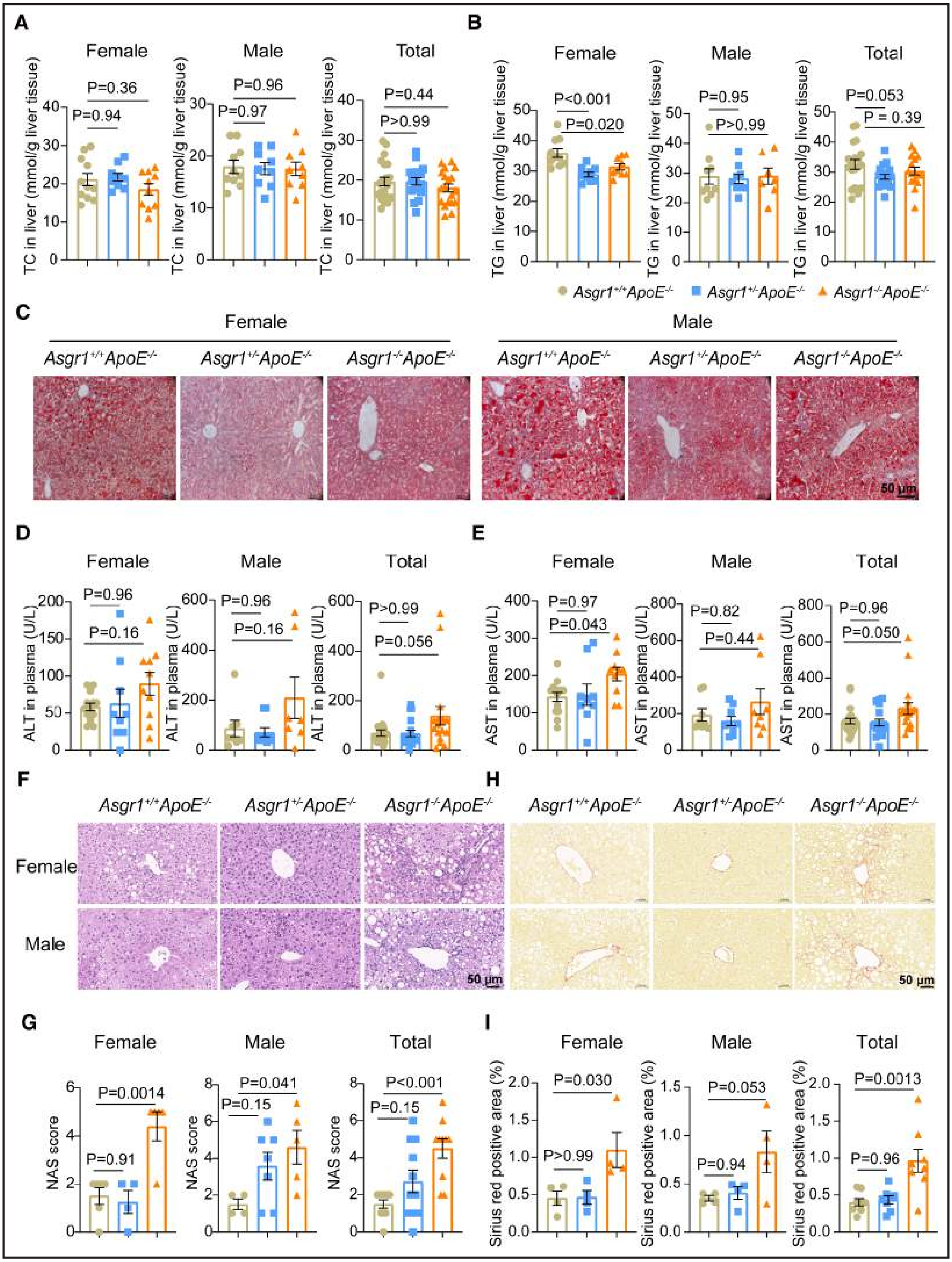

Figure 3. Effects of ASGR1 (asialoglycoprotein receptor 1) deficiency on liver lipid accumulation and liver injury in *ApoE*$^{-/-}$ mice fed a Western diet (WD).

Eight-week-old *Asgr1*$^{+/+}$*ApoE*$^{-/-}$, *Asgr1*$^{+/-}$*ApoE*$^{-/-}$, and *Asgr1*$^{-/-}$*ApoE*$^{-/-}$ mice fed a WD for 12 weeks. **A** and **B**, Total cholesterol (TC; **A**) and triglyceride (TG; **B**) contents in the liver. Female *Asgr1*$^{+/+}$*ApoE*$^{-/-}$, n=10 or 11; female *Asgr1*$^{+/-}$*ApoE*$^{-/-}$, n=9; female *Asgr1*$^{-/-}$*ApoE*$^{-/-}$, n=9 or 10. Male *Asgr1*$^{+/+}$*ApoE*$^{-/-}$, n=9 or 10; male *Asgr1*$^{+/-}$*ApoE*$^{-/-}$, n=9; male *Asgr1*$^{-/-}$*ApoE*$^{-/-}$, n=7 or 9. Total *Asgr1*$^{+/+}$*ApoE*$^{-/-}$, n=19 or 21; total *Asgr1*$^{+/-}$*ApoE*$^{-/-}$, n=18; total *Asgr1*$^{-/-}$*ApoE*$^{-/-}$, n=16 or 19. **C**, Representative oil red O (ORO) staining images of the liver. Bar lengths, 50 μm. **D** and **E**, ALT (alanine aminotransferase; **D**) and AST (aspartate aminotransferase; **E**) in plasma. Female *Asgr1*$^{+/+}$*ApoE*$^{-/-}$, (*Continued*) those in the *Asgr1*$^{+/+}$ group (Figure S4A and S4D), while the ORO and H&E staining results were similar (Figure S4B and S4C). However, there were no significant differences in plasma ALT, AST, H&E, ORO, and sirius red staining results both in ND-fed (Figure S5) or high-fat and high-cholesterol diet–fed (Figure S6) *Asgr1*$^{+/+}$, *Asgr1*$^{+/-}$, and *Asgr1*$^{-/-}$ mice.

Taken together, these results indicate that global ASGR1 deficiency in WD-induced *Asgr1*$^{-/-}$*ApoE*$^{-/-}$ mice and HFD-induced *Asgr1*$^{-/-}$ mice causes liver injury.

ASGR1 Overexpression Increases Atherosclerotic Lesions in WD-Fed *ApoE*$^{-/-}$ Mice

Because ASGR1 deficiency ameliorates atherosclerosis, we next asked whether ASGR1 overexpression increases atherosclerotic lesions. We first constructed an ASGR1-expressing AAV (AAV8-ASGR1; Figure 4A) and demonstrated that the protein level of ASGR1 sharply increased in AML12 cells transfected with AAV8-ASGR1 compared with AAV8-Con (Figure 4B). ASGR1-overexpressing mice were then generated by tail vein injection of AAV8-ASGR1 to both female and male *ApoE*$^{-/-}$ mice, and then the mice were fed a WD for 12 weeks (Figure 4C). Female and male *ApoE*$^{-/-}$ control mice injected with AAV-Con via the tail vein were also fed a WD. Compared with *ApoE*$^{-/-}$+AAV-Con mice, ASGR1-overexpressing *ApoE*$^{-/-}$ mice (*ApoE*$^{-/-}$+AAV-ASGR1) sharply increased the protein level of ASGR1 in the liver tissues but not in other organs (Figure S7). *ApoE*$^{-/-}$+AAV-ASGR1 mice showed an increased lesion burden in the aortic arch in female (P=0.20), male (P=0.20), and total (P=0.071) mice compared with that in the *ApoE*$^{-/-}$+AAV-Con group but without significant changes (Figure 4D). Importantly, the lesion areas in the whole en face aorta were significantly increased in *ApoE*$^{-/-}$+AAV-ASGR1 mice compared with that in the *ApoE*$^{-/-}$+AAV-Con group in both sexes (Figure 4E). In addition, H&E and ORO staining results also showed that ASGR1-overexpressing mice had significantly more lesions in the aortic sinuses than mice in the *ApoE*$^{-/-}$+AAV-Con group (Figure 4F). All ORO-stained en face aorta images and all ORO- and H&E-stained aortic sinus cryosections are shown in Figures S8 and S9. Taken together, these results indicate that ASGR1 overexpression aggravates atherosclerotic lesions in *ApoE*$^{-/-}$ mice, and no apparent differences were observed between male and female mice.

Overexpression of ASGR1 Increases VLDL-C and LDL-C Levels in WD-Fed *ApoE*$^{-/-}$ Mice

The mean body weight of the *ApoE*$^{-/-}$+AAV-Con mice was 28.50 g and that of *ApoE*$^{-/-}$+AAV-ASGR1 mice was 27.88 g, indicating that overexpression of ASGR1 did not affect body weight (Figure 5A). We next determined the plasma and liver lipid levels in ASGR1-overexpressing *ApoE*$^{-/-}$ mice and *ApoE*$^{-/-}$+AAV-Con mice. To be specific, there were no changes in the plasma TC, TG, and glucose levels between *ApoE*$^{-/-}$+AAV-ASGR1 and *ApoE*$^{-/-}$+AAV-Con mice of either sex (Figure 5B through 5D). However, the FPLC assay results showed that the cholesterol contents in VLDLs and LDLs were increased in *ApoE*$^{-/-}$+AAV-ASGR1 compared with that of *ApoE*$^{-/-}$+AAV-Con mice (Figure 5E). Consistent with the trends in the lipoprotein results, the protein levels of ApoB were increased in plasma fractions 17 to 21, which correspond to VLDL lipoproteins, in both female and male *ApoE*$^{-/-}$+AAV-ASGR1 mice compared with *ApoE*$^{-/-}$+AAV-Con mice (Figure 5E).

Overexpression of ASGR1 Mitigates Liver Injury in WD-Fed *ApoE*$^{-/-}$ Mice

Next, we measured liver lipid levels and liver function indices. Compared with *ApoE*$^{-/-}$+AAV-Con mice, the overexpression of ASGR1 did not affect the liver TC and TG contents (Figure 6A and 6B). ORO staining of the liver sections also showed no lipid accumulation changes between the *ApoE*$^{-/-}$+AAV-ASGR1 and *ApoE*$^{-/-}$+AAV-Con mice (Figure 6C). The plasma ALT level was significantly decreased in female and total AAV-ASGR1 mice but not in male AAV-ASGR1 mice compared with AAV-Con mice (Figure 6D). There were no obvious changes in plasma AST levels between the 2 groups in both sexes (Figure 6E). H&E staining results of the liver sections showed that male and total *ApoE*$^{-/-}$+AAV-ASGR1 mice had significantly improved liver morphology compared with *ApoE*$^{-/-}$+AAV-Con mice (Figure 6F). Sirius red staining results showed that the liver fibrosis was significantly alleviated in total *ApoE*$^{-/-}$+AAV-ASGR1 mice (Figure 6G). TUNEL staining results showed that ASGR1 overexpression had no obvious effects on hepatocyte apoptosis (P=0.055; Figure S10). The above data demonstrate that the overexpression of ASGR1 mitigates liver injury in total WD-fed *ApoE*$^{-/-}$ mice.

Figure 3 Continued. n=13 or 14; female *Asgr1*$^{+/-}$*ApoE*$^{-/-}$, n=9; female *Asgr1*$^{-/-}$*ApoE*$^{-/-}$, n=10. Male *Asgr1*$^{+/+}$*ApoE*$^{-/-}$, n=8; male *Asgr1*$^{+/-}$*ApoE*$^{-/-}$, n=9; male *Asgr1*$^{-/-}$*ApoE*$^{-/-}$, n=7 or 8. Total *Asgr1*$^{+/+}$*ApoE*$^{-/-}$, n=21 or 22; total *Asgr1*$^{+/-}$*ApoE*$^{-/-}$, n=18; total *Asgr1*$^{-/-}$*ApoE*$^{-/-}$, n=17 or 18. **F** through **I**, Representative images and quantification results of hematoxylin and eosin (H&E) staining (**F** and **G**) and sirius red (**H** and **I**) staining in liver paraffin sections. Bar lengths, 50 μm. Nonalcoholic fatty liver disease activity score (NAS) and sirius red–positive area were calculated as described in Methods. **G**, Female *Asgr1*$^{+/+}$*ApoE*$^{-/-}$, n=6; female *Asgr1*$^{+/-}$*ApoE*$^{-/-}$, n=4; female *Asgr1*$^{-/-}$*ApoE*$^{-/-}$, n=5. Male *Asgr1*$^{+/+}$*ApoE*$^{-/-}$, n=4; male *Asgr1*$^{+/-}$*ApoE*$^{-/-}$, n=7; male *Asgr1*$^{-/-}$*ApoE*$^{-/-}$, n=5. Total *Asgr1*$^{+/+}$*ApoE*$^{-/-}$, n=10; total *Asgr1*$^{+/-}$*ApoE*$^{-/-}$, n=11; total *Asgr1*$^{-/-}$*ApoE*$^{-/-}$, n=10. **I**, n=4 mice for each female and male group; n=8 mice for each total group. Data were statistically analyzed by 1-way ANOVA compared with *Asgr1*$^{+/+}$*ApoE*$^{-/-}$ mice, and the values are expressed as mean±SEM.

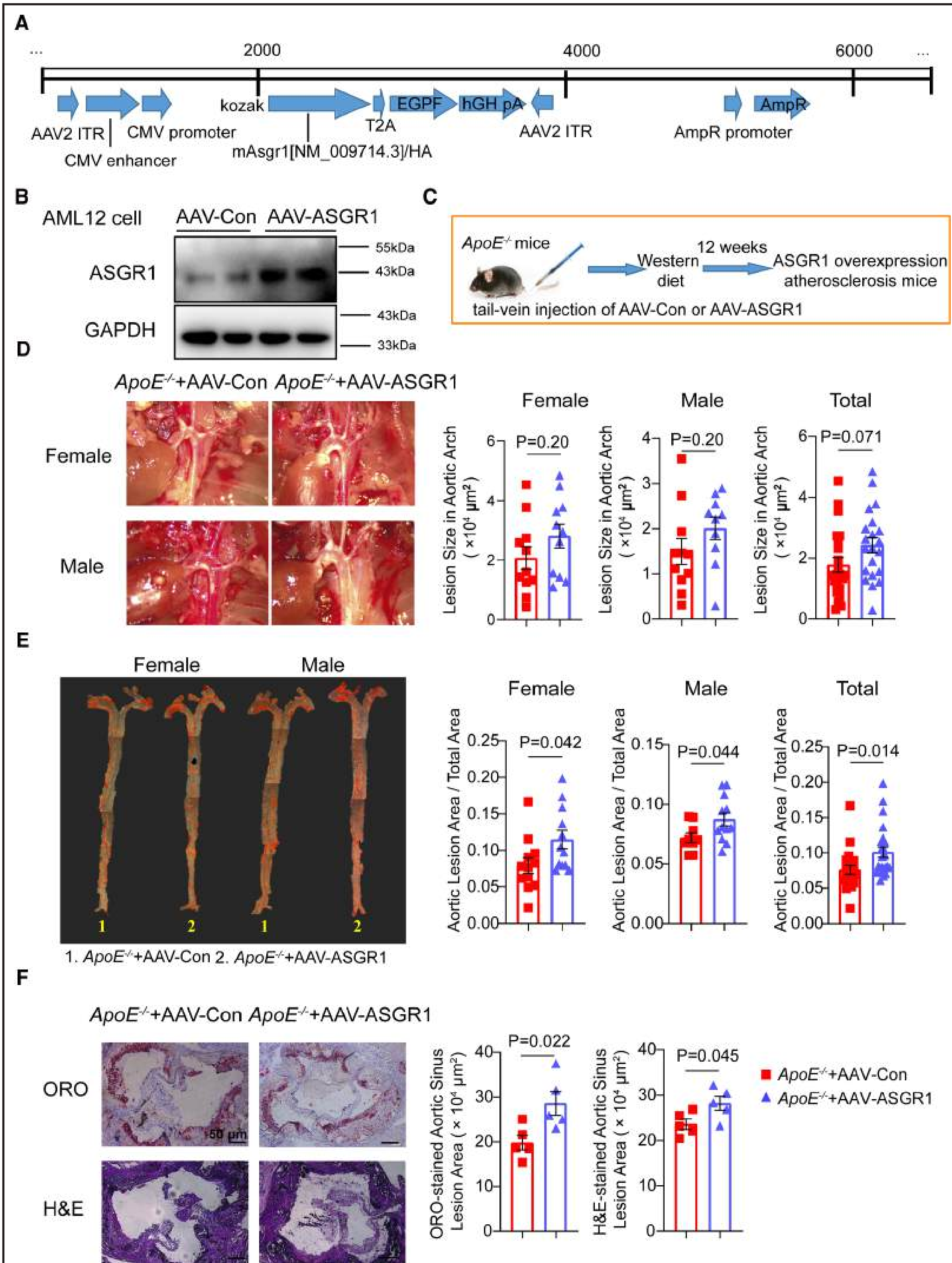

Figure 4. ASGR1 (asialoglycoprotein receptor 1) overexpression aggravates atherogenesis in Western diet (WD)–fed *ApoE*$^{-/-}$ mice.

A, Schematic showing the generation of the ASGR1 overexpression vector. **B**, α-Mouse liver 12 (AML12) cells were transfected with AAV8-ASGR1 or AAV8-Con virus for 48 hours, and the ASGR1 protein level was analyzed by Western blotting. **C**, Schematic showing the generation of ASGR1-overexpressing *ApoE*$^{-/-}$ mice. Eight-week-old male and female *ApoE*$^{-/-}$ mice were injected with 1×10^{11} GC (genomic copies) of AAV8-ASGR1 or AAV8-Con (n=12 per group) through the tail vein and fed a WD for 12 weeks. **D**, Representative images of the (*Continued*)

ASGR1 Deficiency Decreases VLDL Production by Inhibiting MTTP and ANGPTL3/8 Expression and Increasing LPL Activity

Generally, a combination of lipoproteins VLDL, IDL, and LDL contribute to the amount of cholesterol deposited in the arterial wall and hence promote the progression of atherosclerosis.[27] It was reported that *Asgr1*$^{-/-}$ mice had a defect in VLDL/LDL secretion compared with wild-type mice (*Asgr1*$^{+/+}$).[14] Because the cholesterol levels in plasma lipoproteins VLDL and LDL were significantly reduced in ASGR1$^{-/-}$ *ApoE*$^{-/-}$ mice but increased in ASGR1-overexpressing *ApoE*$^{-/-}$ mice according to the plasma FPLC results (Figures 2 and 5), we speculated that deficiency or overexpression of ASGR1 in *ApoE*$^{-/-}$ mice may influence VLDL secretion and clearance.

To test our hypothesis, we first measured the plasma TG levels to determine the secretion rate of VLDL-TG at 1, 2, and 3 hours after administration of the LPL inhibitor tyloxapol. As shown in Figure 7A, the plasma TG levels of *Asgr1*$^{+/-}$*ApoE*$^{-/-}$ and *Asgr1*$^{-/-}$*ApoE*$^{-/-}$ mice were lower than that of *Asgr1*$^{+/+}$*ApoE*$^{-/-}$ mice, and the most significant difference was observed at 3 hours after tail vein injection with tyloxapol (*Asgr1*$^{+/-}$*ApoE*$^{-/-}$ decreased by 20.81%, P=0.0083; *Asgr1*$^{-/-}$*ApoE*$^{-/-}$ decreased by 29.07%, P<0.001); however, the plasma TG level of *ApoE*$^{-/-}$+AAV-ASGR1 mice was higher than that of *ApoE*$^{-/-}$+AAV-Con mice at 2 hours (increased by 39.46%) and 3 hours (increased by 53.15%; P<0.001) after injection with tyloxapol (Figure 7A). In addition, within 3 hours after injection with tyloxapol, the plasma TC levels did not show a significant difference between the groups of *Asgr1*$^{+/-}$*ApoE*$^{-/-}$ and *Asgr1*$^{-/-}$*ApoE*$^{-/-}$ mice compared with *Asgr1*$^{+/+}$*ApoE*$^{-/-}$ or *ApoE*$^{-/-}$+AAV-ASGR1 mice compared with *ApoE*$^{-/-}$+AAV-Con mice (Figure 7B). Because the mice were fasted for 12 hours in the present study, the rise of plasma TG levels should be due to VLDL.[28] In addition, ND-fed *Asgr1*$^{-/-}$ mice also decreased VLDL-TG secretion rate compared with *Asgr1*$^{+/+}$ mice (Figure S11). Together, these results reveal that ASGR1 deficiency lowers VLDL-TG secretion, while ASGR1 overexpression increases VLDL-TG secretion.

The assembly and secretion of hepatic VLDL is critically dependent on the coordinated interactions of 2 dominant proteins, namely MTTP and ApoB.[29] We determined whether the ASGR1-mediated effects on VLDL secretion are related to MTTP and ApoB. qRT-PCR results showed that the mRNA levels of *Mttp* were decreased in *Asgr1*$^{+/-}$*ApoE*$^{-/-}$ (P=0.25) and *Asgr1*$^{-/-}$*ApoE*$^{-/-}$ (P=0.054) mice but with no significant differences compared with that in *Asgr1*$^{+/+}$*ApoE*$^{-/-}$ mice (Figure 7C), and the mRNA levels of *ApoB* were not altered (Figure 7C). There were no significant changes in the mRNA levels of *Mttp* and *ApoB* in *ApoE*$^{-/-}$+AAV-ASGR1 mice compared with *ApoE*$^{-/-}$+AAV-Con mice (Figure 7D). Strikingly, the protein level of MTTP significantly reduced in *Asgr1*$^{+/-}$*ApoE*$^{-/-}$ and *Asgr1*$^{-/-}$*ApoE*$^{-/-}$ mice when compared with *Asgr1*$^{+/+}$*ApoE*$^{-/-}$ mice but increased in ASGR1-overexpressing mice when compared with *ApoE*$^{-/-}$+AAV-Con mice (Figure 7E and 7F), indicating that ASGR1 deficiency inhibits VLDL synthesis and secretion and thus reduces the plasma circulating VLDL levels by inhibiting MTTP.

LPL catalyzes intravascular hydrolysis of the TG core of circulating TG-rich lipoproteins, such as CMs and VLDL, which is a central event in lipid metabolism.[30,31] Modulation of LPL activity correlates with the risk of CVD events. Previous studies demonstrate that the enzyme activity of LPL is inhibited by ANGPTL3 (angiopoietin-like protein 3), ANGPTL4 (angiopoietin-like protein 4), and ANGPTL8 (angiopoietin-like protein 8).[30,31] We tested LPL activity in the plasma and ANGPTL3/4/8 expression in the liver to determine whether ASGR1 affects LPL activity. Notably, *Asgr1*$^{-/-}$*ApoE*$^{-/-}$ mice had significant increased LPL activity compared with *Asgr1*$^{+/+}$*ApoE*$^{-/-}$ mice, while *ApoE*$^{-/-}$+AAV-ASGR1 mice showed significantly inhibited LPL activity compared with *ApoE*$^{-/-}$+AAV-Con mice (Figure 7G). In addition, *Asgr1*$^{-/-}$*ApoE*$^{-/-}$ mice had significantly increased HL (hepatic lipase) compared with *Asgr1*$^{+/+}$*ApoE*$^{-/-}$ mice (P=0.015), while *ApoE*$^{-/-}$+AAV-ASGR1 mice showed an inhibited HL activity compared with *ApoE*$^{-/-}$+AAV-Con mice but with no significant differences (P=0.11; Figure S12). The protein expression levels of ANGPTL3 were significantly decreased in both *Asgr1*$^{+/-}$*ApoE*$^{-/-}$ and *Asgr1*$^{-/-}$*ApoE*$^{-/-}$ mice when compared with *Asgr1*$^{+/+}$*ApoE*$^{-/-}$ mice but increased in ASGR1-overexpressing mice when compared with *ApoE*$^{-/-}$+AAV-Con mice (Figure 7E and 7F). Furthermore, qRT-PCR results showed that the mRNA levels of *Angptl8*, but not *Angptl3/4*, were significantly decreased in *Asgr1*$^{+/-}$*ApoE*$^{-/-}$ and *Asgr1*$^{-/-}$*ApoE*$^{-/-}$ mice compared with that in *Asgr1*$^{+/+}$*ApoE*$^{-/-}$ mice (Figure 7H), while the mRNA levels of *Angptl3* (P=0.063) and *Angptl8* (P=0.080) were slightly increased in *ApoE*$^{-/-}$+AAV-ASGR1 mice compared with *ApoE*$^{-/-}$+AAV-Con mice (Figure 7I). In addition, the in vitro assay results showed

Figure 4 Continued. aortic arch in situ. The bar diagrams show the statistical evaluation of the lesion size in the aortic arch with the ImageJ software (female *ApoE*$^{-/-}$+AAV-Con, n=11; female *ApoE*$^{-/-}$+AAV-ASGR1, n=11; male *ApoE*$^{-/-}$+AAV-Con, n=11; male *ApoE*$^{-/-}$+AAV-ASGR1, n=10; total *ApoE*$^{-/-}$+AAV-Con, n=22; total *ApoE*$^{-/-}$+AAV-ASGR1, n=21). **E**, Representative en face view of oil red O (ORO)–stained aortas. Lesion sizes were quantitatively analyzed with the ImageJ software (female *ApoE*$^{-/-}$+AAV-Con, n=12; female *ApoE*$^{-/-}$+AAV-ASGR1, n=12; male *ApoE*$^{-/-}$+AAV-Con, n=9; male *ApoE*$^{-/-}$+AAV-ASGR1, n=12; total *ApoE*$^{-/-}$+AAV-Con, n=21; total *ApoE*$^{-/-}$+AAV-ASGR1, n=24). **F**, ORO and hematoxylin and eosin (H&E) staining of aortic sinus cross sections. Lesion sizes were quantitatively analyzed with the ImageJ software (n=5 for ORO staining for each group; n=5 for H&E staining for each group). Bar lengths, 50 μm. Data were statistically analyzed using the Student *t* test compared with the *ApoE*$^{-/-}$+AAV-Con group, and the values are expressed as mean±SEM. AAV indicates adeno-associated virus.

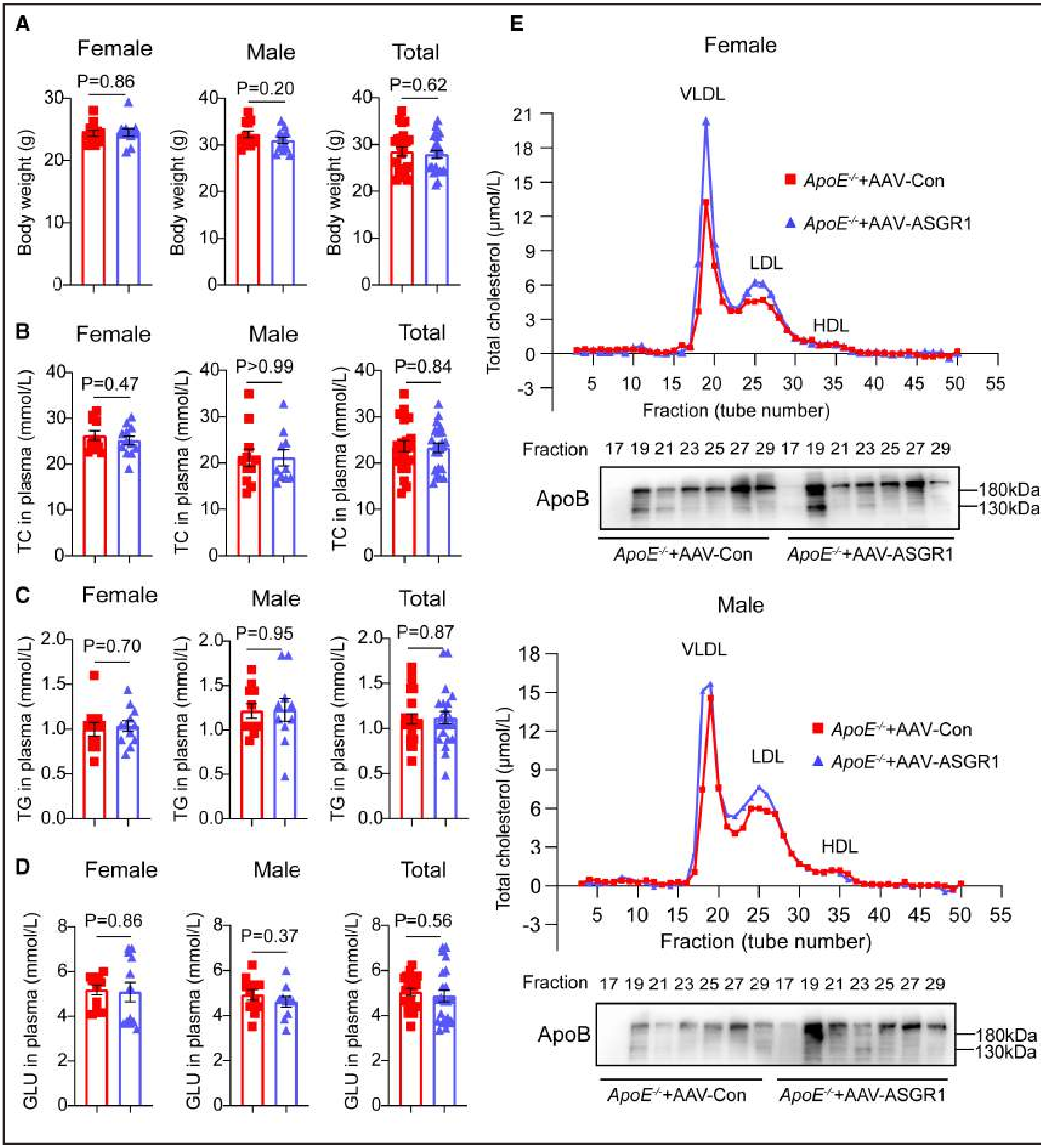

Figure 5. Effects of ASGR1 (asialoglycoprotein receptor 1) overexpression on lipid profiles in *ApoE*$^{-/-}$ mice fed a Western diet (WD).

A through **D**, Body weight (**A**), plasma total cholesterol (TC; **B**), plasma triglyceride (TG; **C**), and glucose (GLU; **D**) levels of 8-week-old *ApoE*$^{-/-}$+AAV-Con and *ApoE*$^{-/-}$+AAV-ASGR1 mice fed a WD for 12 weeks. Female or male *ApoE*$^{-/-}$+AAV-Con, n=10 or 11 for each group; female or male *ApoE*$^{-/-}$+AAV-ASGR1, n=10 to 12 for each group. Total *ApoE*$^{-/-}$+AAV-Con or *ApoE*$^{-/-}$+AAV-ASGR1, n=22 or 23 for each group. **E**, Plasma cholesterol distribution and ApoB protein expression. Plasma was pooled from each group (n=10–12), and the distribution of plasma cholesterol in different types of lipoproteins was determined after separation by fast protein liquid chromatography (FPLC). Protein expression levels of ApoB in the fractions of female and male *ApoE*$^{-/-}$+AAV-Con and *ApoE*$^{-/-}$+AAV-ASGR1 mice were analyzed by Western blotting. Data were statistically analyzed by Student *t* test analysis, and the values are expressed as mean±SEM. *P* values were calculated by comparison with the *ApoE*$^{-/-}$+AAV-Con group. AAV indicates adeno-associated virus.

that the mRNA expression levels of *Mttp*, *Angptl3*, and *Angptl8* were significantly decreased when *Asgr1* was knocked down compared with its own control in HepG2 cells (Figure S13). These above results suggest that ASGR1 deficiency increases VLDL-TG clearance by inhibiting ANGPTL3/8 and increasing LPL activity.

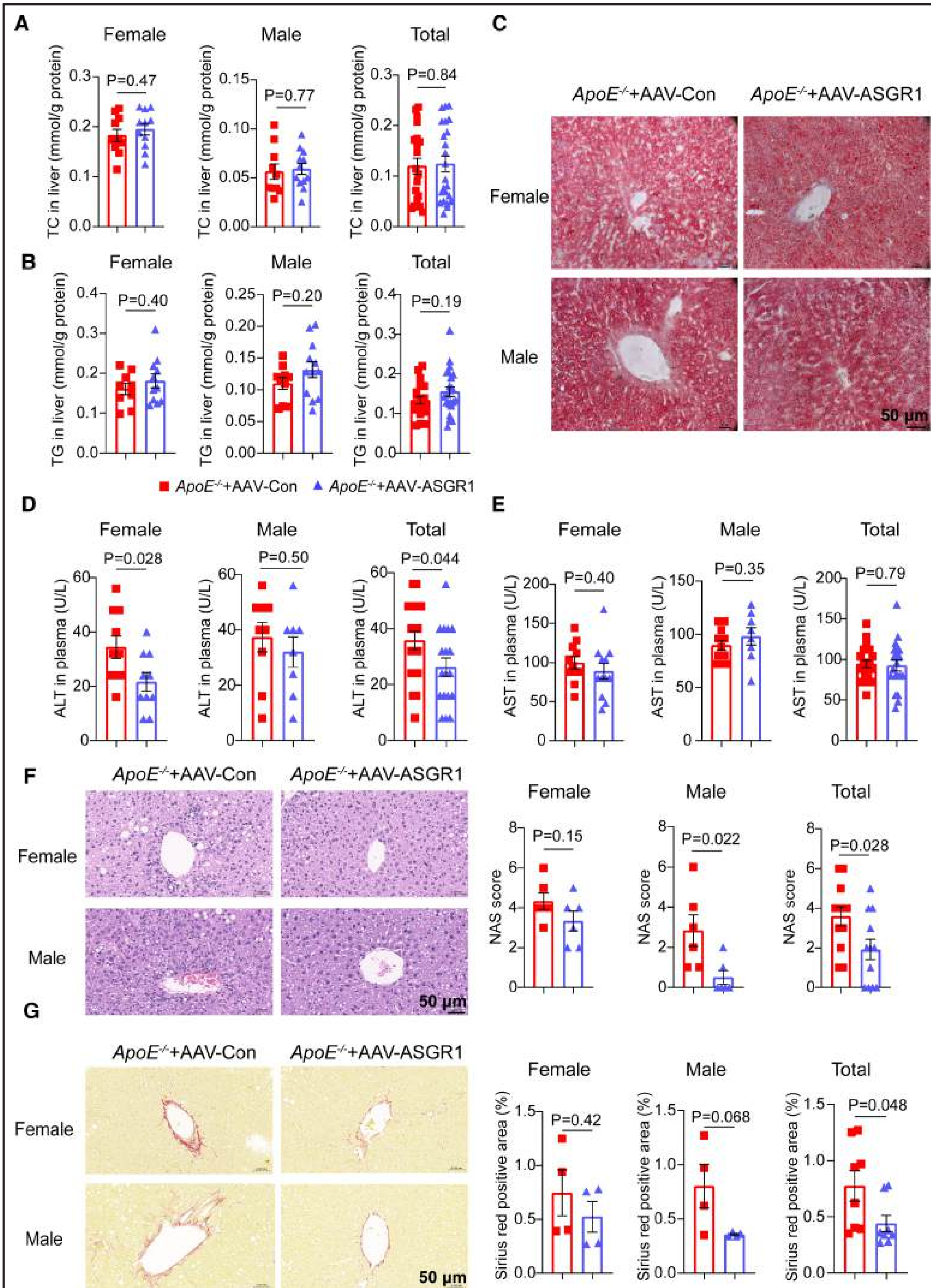

Figure 6. Effects of ASGR1 (asialoglycoprotein receptor 1) overexpression on lipid accumulation and liver injury in livers in *ApoE*$^{-/-}$ mice fed a Western diet (WD).

Eight-week-old *ApoE*$^{-/-}$+AAV-Con and *ApoE*$^{-/-}$+AAV-ASGR1 mice fed a WD for 12 weeks. **A** and **B**, Total cholesterol (TC; **A**) and triglyceride (TG; **B**) contents in the liver (male or female *ApoE*$^{-/-}$+AAV-Con mice, n=9 or 10 for each group; male or female *ApoE*$^{-/-}$+AAV-ASGR1 mice, n=11 or 12 for each group; total *ApoE*$^{-/-}$+AAV-Con or *ApoE*$^{-/-}$+AAV-ASGR1 mice, n=19–23 for each group). **C**, Representative oil red O (ORO) staining images of the liver. Bar lengths, 50 μm. **D** and **E**, ALT (alanine aminotransferase; **D**) and AST (aspartate (*Continued*)

Together, our results suggest that ASGR1 deficiency decreases VLDL-TG production by inhibiting MTTP and ANGPTL3/8 expression and increasing LPL activity.

ASGR1 Deficiency Promotes Cholesterol Excretion by Regulating Cholesterol Metabolism–Associated Gene Expression

Cholesterol efflux is one of the main regulatory mechanisms that prevents atherosclerosis.[32] Recently, Wang et al[15] found that inhibition of ASGR1 could decrease lipid levels by promoting cholesterol excretion compared with *Asgr1*$^{+/+}$ mice. We tested whether the antiatherosclerotic effect of ASGR1 deficiency in WD-fed *ApoE*$^{-/-}$ mice was related to cholesterol efflux. The results showed that cholesterol contents in feces from WD-fed *Asgr1*$^{+/-}$*ApoE*$^{-/-}$ and *Asgr1*$^{-/-}$*ApoE*$^{-/-}$ mice were significantly increased compared with WD-fed *Asgr1*$^{+/+}$*ApoE*$^{-/-}$ mice (Figure 8A). However, the cholesterol content in feces from WD-fed *ApoE*$^{-/-}$ mice was significantly decreased when ASGR1 was overexpressed (Figure 8A). Moreover, biliary TC significantly increased in *Asgr1*$^{-/-}$*ApoE*$^{-/-}$ mice compared with the *Asgr1*$^{+/+}$*ApoE*$^{-/-}$ group (Figure S14). These data indicate that ASGR1 deficiency may promote cholesterol efflux and thus inhibit the development of atherosclerosis.

The process of cholesterol efflux is mediated by transporters such as ABCA1,[33] ABCG5,[34] LXRα,[35] CYP7A1,[36,37] and others. CYP7A1 is the rate-limiting enzyme in the conversion of cholesterol to bile acids in the liver.[36–38] INSIG1 negatively regulates the transcriptional function of SREBP, which is the key protein of lipidogenesis.[39] *ACC* (acetyl-CoA carboxylase) is a key regulatory gene for lipid synthesis. AMPK (AMP-activated protein kinase) is a central regulator of energy homeostasis,[40] and it can inhibit fatty acid synthesis through phosphorylation and inactivation of ACC.[41,42] The levels of these proteins were measured by Western blotting in the livers of both *Asgr1*$^{-/-}$ and ASGR1-overexpressing *ApoE*$^{-/-}$ mice. The protein expression levels of ASGR1 decreased in *Asgr1*$^{-/-}$*ApoE*$^{-/-}$ mice (Figure 8B) but increased in ASGR1-overexpressing *ApoE*$^{-/-}$ mice (Figure 8C), which means that ASGR1 was successfully knocked out or overexpressed. The protein levels of LDLR, ABCA1, ABCG5, LXRα, CYP7A1, and phosphorylated AMPK were significantly increased in the livers of *Asgr1*$^{-/-}$*ApoE*$^{-/-}$ mice compared with *Asgr1*$^{+/+}$*ApoE*$^{-/-}$ mice (Figure 8B) but decreased in ASGR1-overexpressing *ApoE*$^{-/-}$ mice compared with the *ApoE*$^{-/-}$+AAV-Con mice (Figure 8C). These above data may explain why ASGR1 deficiency increases fecal cholesterol content. Although the protein levels of phosphorylated AMPK were significantly increased, phosphorylated ACC was significantly decreased and ACC significantly increased in the livers of *Asgr1*$^{-/-}$*ApoE*$^{-/-}$ mice (Figure 8B); in contrast, phosphorylated ACC was significantly increased in the livers of ASGR1-overexpressing *ApoE*$^{-/-}$ mice, and ACC significantly decreased (Figure 8C). The effect of ASGR1 on ACC might lead to lipid accumulation in *Asgr1*$^{-/-}$ mice (Figure 3).

To explore the underlying mechanisms of ASGR1-mediated effects in atherosclerosis, RNA-sequencing analysis of liver tissues of *Asgr1*$^{+/+}$, *Asgr1*$^{+/-}$, and *Asgr1*$^{-/-}$ mice was performed. The DEGs expressed in *Asgr1*$^{+/-}$ and *Asgr1*$^{-/-}$ mice were compared with *Asgr1*$^{+/+}$ mice (Figure 9A and 9B). The results showed that 326 genes were significantly changed (fold change, >2; $P<0.05$) in *Asgr1*$^{+/-}$ versus *Asgr1*$^{+/+}$ mice, among which 163 genes were downregulated and 163 genes were upregulated in *Asgr1*$^{+/-}$ mice (Figure 9A and 9B). In *Asgr1*$^{-/-}$ mice, 167 genes were significantly changed (fold change, >2; $P<0.05$), among which 73 genes were downregulated and 94 genes were upregulated compared with *Asgr1*$^{+/+}$ mice (Figure 9A and 9B). Among these DEGs, 98 were the same in *Asgr1*$^{+/-}$ and *Asgr1*$^{-/-}$ versus *Asgr1*$^{+/+}$ mice (Figure 9A). Gene ontology pathway analysis showed that these DEGs mainly belong to lipid metabolism or catabolism processes, cholesterol metabolism, bile acid biosynthesis or secretion, and fatty acid oxidation, biosynthesis, or metabolism (Figure 9C). Notably, ASGR1 deficiency decreased the expression of atherogenic genes (such as *Asgr1*, *Ces4a*, *Elovl3*, *Fabp5*, *Sort1*, *Slcola1*, and *Nr0b2*), while upregulating multiple atheroprotective genes (such as *Cyp46a1*, *Vldlr*, *Sult2a1*, *Sult2a2*, *Sult2a3*, *Sult2a6*, *Hao2*, *Per2*, *Acot3*, and *Eci3*; Figure 9D). Taken together, these findings indicate that ASGR1 is vital in the regulatory network of lipid and cholesterol homeostasis, and the schematic of the role of ASGR1 in atherosclerosis is shown in Figure 9E.

DISCUSSION

Atherosclerosis is the leading cause of mortality and morbidity worldwide. Clinical studies indicate that loss of ASGR1 function is significantly associated with lower non–HDL-C levels and reduces CAD risks, suggesting that ASGR1 may contribute to the development and progression of atherosclerosis. In this study,

Figure 6 Continued. aminotransferase; **E**) in plasma (male or female *ApoE*$^{-/-}$+AAV-Con mice, n=9–11 for each group; male or female *ApoE*$^{-/-}$+AAV-ASGR1 mice, n=8–12 for each group; total *ApoE*$^{-/-}$+AAV-Con or *ApoE*$^{-/-}$+AAV-ASGR1 mice, n=18–22 for each group.). **F** and **G**, Representative images and quantification of hematoxylin and eosin (H&E; **F**) and sirius red (**G**) staining of the liver sections. n=4 or 6 for male or female *ApoE*$^{-/-}$+AAV-Con and *ApoE*$^{-/-}$+AAV-ASGR1 mice. n=8 or 12 for total *ApoE*$^{-/-}$+AAV-Con and *ApoE*$^{-/-}$+AAV-ASGR1 mice. Bar lengths, 50 μm. Data were statistically analyzed by the Student *t* test compared with the *ApoE*$^{-/-}$+AAV-Con group, and the values are expressed as mean±SEM. AAV indicates adeno-associated virus.

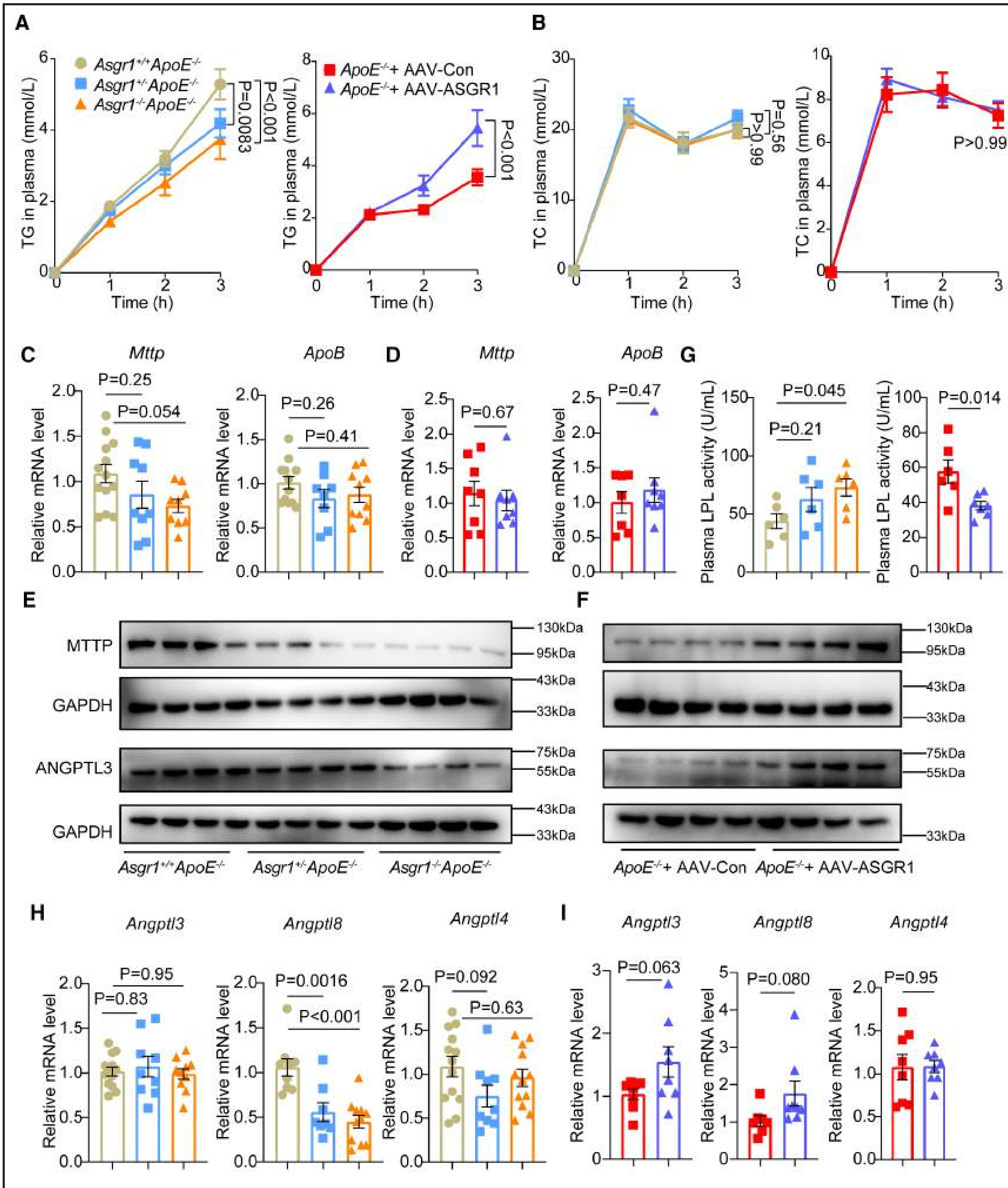

Figure 7. ASGR1 (asialoglycoprotein receptor 1) increases VLDL (very-low-density lipoprotein) production and inhibits LPL (lipoprotein lipase) activity by affecting MTTP (microsomal triglyceride transfer protein) and ANGPTL3/8 (angiopoietin-like protein 3/8) expression.

A and **B**, The triglyceride (TG) and total cholesterol (TC) content in the plasma at the first, second, and third hours after injection with tyloxapol (*Asgr1*$^{+/+}$*ApoE*$^{-/-}$ mice, n=7; *Asgr1*$^{+/-}$*ApoE*$^{-/-}$ mice, n=8; *Asgr1*$^{-/-}$*ApoE*$^{-/-}$ mice, n=5; *ApoE*$^{-/-}$+AAV-Con mice, n=6; *ApoE*$^{-/-}$+AAV-ASGR1 mice, n=5). **C** and **D**, Relative mRNA levels of *Mttp* and *ApoB* analyzed by quantitative real-time polymerase chain reaction (qRT-PCR). **E** and **F**, Relative protein levels of MTTP and ANGPTL3 in the liver analyzed by Western blotting. **G**, Lipoprotein lipase (LPL) activity in the plasma (n=6 or 7 for each group). **H** and **I**, Relative mRNA levels of *Angptl3/8/4* analyzed by qRT-PCR. The values are expressed as mean±SEM. **C** and **H**, n=8 to 13 for each group. **D** and **I**, n=7 or 8 for each group. **A** and **B**, Data were statistically analyzed by 2-way ANOVA. **C**, **D**, **G**, **H**, and **I**, Data were statistically analyzed by 1-way ANOVA compared with *Asgr1*$^{+/+}$*ApoE*$^{-/-}$ mice or the Student *t* test compared with the *ApoE*$^{-/-}$+AAV-Con group. AAV indicates adeno-associated virus.

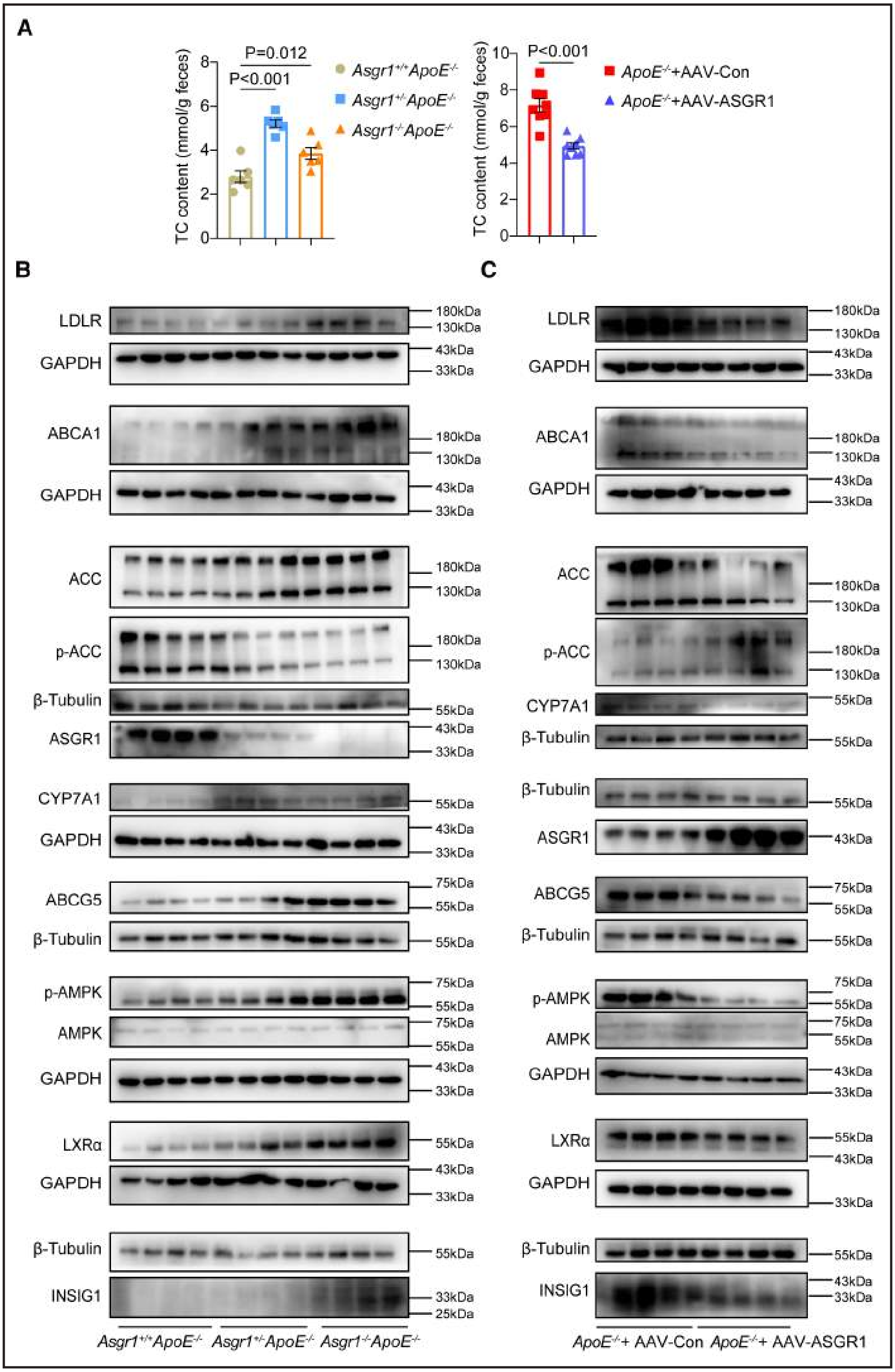

Figure 8. ASGR1 (asialoglycoprotein receptor 1) inhibits cholesterol efflux and regulates the levels of key proteins related to lipid and cholesterol metabolism in livers from atherosclerosis mice.

A, Total cholesterol (TC) content in feces. *Asgr1*$^{-/-}$ or ASGR1-overexpressing *ApoE*$^{-/-}$ mice fed a Western diet (WD) for 12 weeks (n=6–8). Data were expressed as mean±SEM. Data were statistically analyzed by 1-way ANOVA analysis compared with *Asgr1*$^{+/+}$*ApoE*$^{-/-}$ mice or Student *t* test compared with the *ApoE*$^{-/-}$+AAV-Con group. **B** and **C**, The levels of key proteins related to lipid and cholesterol metabolism in livers were analyzed by Western blotting. The protein samples from 8 mice of each group were pooled. Representative images are shown with 4 duplicates for each group. AAV indicates adeno-associated virus.

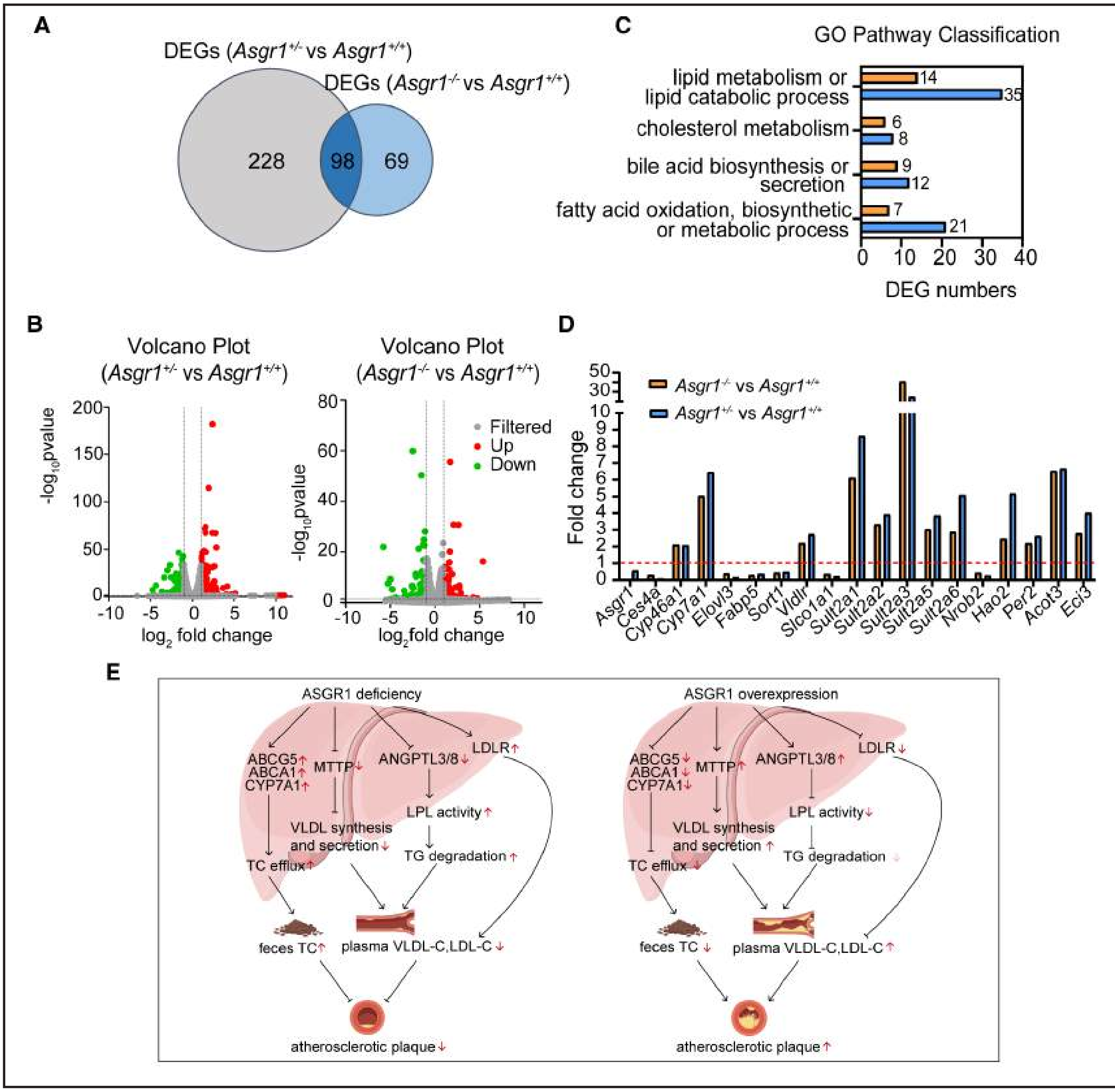

Figure 9. The mechanism of ASGR1 (asialoglycoprotein receptor 1) in atherosclerosis.

A through **D**, The effects of *Asgr1* deficiency on lipid and cholesterol metabolism by the liver. RNA-sequencing analysis (RNA-seq) was performed using livers from 8-week-old male *Asgr1*$^{+/+}$, *Asgr1*$^{+/-}$, and *Asgr1*$^{-/-}$ mice. n=2 for each group. **A**, Venn diagram showing the number of differentially expressed genes (DEGs) in *Asgr1*$^{-/-}$ vs *Asgr1*$^{+/+}$ and *Asgr1*$^{+/-}$ vs *Asgr1*$^{+/+}$ groups. **B**, Volcano plots of DEGs in *Asgr1*$^{+/-}$ vs *Asgr1*$^{+/+}$ groups and *Asgr1*$^{-/-}$ vs *Asgr1*$^{+/+}$ groups. The horizontal coordinate is the fold-change value of genes between *Asgr1*$^{-/-}$ or *Asgr1*$^{+/-}$ vs *Asgr1*$^{+/+}$ mice and the vertical coordinate is the value of −log10(*P* value). The green dots represent downregulated DEGs, red dots represent upregulated DEGs, and gray dots represent nonsignificantly differential genes. **C**, Gene ontology (GO) pathway classification analysis of DEGs in *Asgr1*$^{-/-}$ vs *Asgr1*$^{+/+}$ and *Asgr1*$^{+/-}$ vs *Asgr1*$^{+/+}$ groups. **D**, Fold changes of several DEGs are shown. **E**, Schematic of the role of ASGR1 in atherosclerosis. ASGR1 deficiency alleviates atherosclerosis while ASGR1 overexpression promotes atherosclerosis. Mechanistically, ASGR1 regulates lipoprotein VLDL (very-low-density lipoprotein) and LDL (low-density lipoprotein) metabolism and cholesterol efflux by regulating the activity or expression of key proteins in VLDL synthesis, triglyceride (TG) hydrolysis, LDL uptake, and cholesterol efflux. Specifically, ASGR1 deficiency in *ApoE*$^{-/-}$ mice reduces VLDL secretion by inhibiting MTTP (microsomal triglyceride transfer protein) expression, increases VLDL clearance by inhibiting ANGPTL3/8 (angiopoietin-like protein 3/8) and increasing LPL (lipoprotein lipase) activity, increases LDL uptake in the liver by upregulating LDLR (LDL receptor) protein expression, and promotes cholesterol efflux by upregulating the protein expression of LXRα (liver X receptor-α), ABCA1 (ATP-binding cassette subfamily A member 1), ABCG5 (ATP-binding cassette subfamily G member 5), CYP7A1 (cytochrome P450 family 7 subfamily A member 1), phosphorylated AMP-activated protein kinase (p-AMPK), and INSIG1 (insulin-induced gene 1), thus alleviating the development of atherosclerosis; however, ASGR1 overexpression in *ApoE*$^{-/-}$ mice had an opposite effect, thus promoting the development of atherosclerosis. The schematic diagram of the graphic abstract was drawn by Figdraw.

we comprehensively delineated the role and underlying mechanisms of ASGR1 in atherosclerosis by utilizing both genetic deletion and overexpression of ASGR1 in the classic *ApoE*$^{-/-}$ mouse model of atherosclerosis. Our results demonstrate that ASGR1 deficiency retards atherosclerosis, while ASGR1 overexpression promotes atherosclerosis in WD-fed *ApoE*$^{-/-}$ mice. The mechanisms whereby ASGR1 deficiency inhibits atherosclerosis are related to VLDL synthesis and secretion, TG hydrolysis, LDL uptake, and cholesterol efflux (Figure 9E).

A large body of evidence suggests that disorders of lipid metabolism are central to the development of the pathology of atherosclerosis, and managing LDL-C and non–HDL-C (the cholesterol in all proatherogenic lipoproteins, such as LDL, VLDL, and IDL) levels is a key intervention for the prevention of atherosclerotic CVD.[2,6–8] VLDL is a cholesterol- and TG-rich lipoprotein that is secreted into the bloodstream from the liver, and VLDL can be further metabolized to LDL after removal of their TG.[43,44] The assembly and secretion of hepatic VLDL production in the liver is critically dependent on MTTP and ApoB.[29,45] The TG hydrolysis in VLDL is mediated by LPL[46] whose activity is inhibited by ANGPTL3/4/8.[30,31] In our study, ASGR1 deficiency in *ApoE*$^{-/-}$ mice significantly reduced VLDL production through inhibiting MTTP expression, which is consistent with the results in *Asgr1*$^{-/-}$ mice.[14] However, ASGR1 overexpression in *ApoE*$^{-/-}$ mice increased MTTP protein expression, thus accelerating VLDL synthesis and secretion and promoting atherosclerosis. Importantly, our study demonstrates that ASGR1 deficiency in *ApoE*$^{-/-}$ mice increases VLDL-TG clearance through inhibiting ANGPTL3/8 and increasing LPL activity, while ASGR1 overexpression in *ApoE*$^{-/-}$ mice increases ANGPTL3/8 expression and thus inhibits LPL activity and suppresses TG degradation. In addition, ASGR1 deficiency in *ApoE*$^{-/-}$ mice significantly increased LDLR protein expression, thus increasing LDL uptake in the liver, while ASGR1 overexpression in *ApoE*$^{-/-}$ mice decreased LDLR protein expression. Therefore, the observed VLDL-C and LDL-C decrease and reduced plaques in *Asgr1*$^{-/-}$*ApoE*$^{-/-}$ mice are mainly dependent on the combined effects of ASGR1 on regulating lipoprotein VLDL and LDL metabolism.

Elevated blood cholesterol is strongly related to the development of atherosclerosis and CVD. Reverse cholesterol transport is a pathway that transports accumulated cholesterol from the vessel wall to the liver and finally excretes cholesterol through feces, thus preventing atherosclerosis.[47] ASGR1 regulates cholesterol metabolism.[15] Our data demonstrated that cholesterol contents in feces (Figure 8A) and bile (Figure S14) from WD-fed *Asgr1*$^{-/-}$*ApoE*$^{-/-}$ mice were significantly increased compared with WD-fed *Asgr1*$^{+/+}$*ApoE*$^{-/-}$ mice. However, the cholesterol content in feces from WD-fed *ApoE*$^{-/-}$ mice was significantly decreased when ASGR1 was overexpressed (Figure 8A). These data indicate that ASGR1 deficiency may promote cholesterol efflux and thus inhibit the development of atherosclerosis. LXRα is a sterol sensor that regulates cholesterol homeostasis.[48] Our data showed that ASGR1 deficiency in *ApoE*$^{-/-}$ mice fed a WD positively regulated LXRα and its downstream genes, such as *ABCA1*, *ABCG5*, and *CYP7A1* (Figure 8B), which is consistent with previous studies.[15] However, ASGR1 overexpression in *ApoE*$^{-/-}$ mice fed a WD negatively regulated LXRα and its downstream genes (Figure 8C). The effects of ASGR1 on these key proteins in cholesterol efflux could explain why ASGR1 deficiency or overexpressison affects feces cholesterol contents. What is more, LXRα and CYP7A1 are also important in the conversion of cholesterol to bile acids in the liver to maintain bile acid homeostasis,[36–38,49] and modification of bile acids directly affects the progression of this process.[50] According to the RNA-sequencing results, the expression of *Sult2a* family genes (*Sult2a1*, *Sult2a2*, *Sult2a3*, and *Sult2a6*), which are regulated by LXRs and involved in the modification and regulation of bile acids,[51] was significantly upregulated in the livers of *Asgr1*$^{-/-}$ mice when compared with that in *Asgr1*$^{+/+}$ mice. These data indicate that ASGR1 is likely to affect changes in bile acids in mice. However, we did not detect a significant difference in bile acid levels in the bile of *Asgr1*$^{-/-}$ or ASGR1-overexpressing *ApoE*$^{-/-}$ mice compared with that in control mice (data not shown). Further studies should investigate whether ASGR1 affects the composition of bile acids. Taken together, our data demonstrate that ASGR1 deficiency increases cholesterol efflux and may be another important mechanism to retard atherosclerosis.

ASGR1 is a liver-specific receptor, but the role of ASGR1 in liver injury has not been elucidated and remains controversial. Zhu et al[52] revealed ASGR1 can inhibit liver cancer as a tumor suppressor. Xie et al[19] found *Asgr1*$^{-/-}$ pigs had a lower CVD risk but there was mild-to-moderate liver injury. Shi et al[20] found ASGR1 promoted liver injury by regulating monocyte-to-macrophage differentiation via the NF-κB (nuclear factor-κB)/ATF5 (activating transcription factor 5) pathway in sepsis. Svecla et al[53] revealed that *Asgr1*$^{-/-}$ mice subjected to an HFD for 20 weeks could reduce the plasma lipid level by diverting lipids toward the adipose tissue but results in liver damage during obesity. ASGR1 deficiency promoted acetaminophen-induced acute and CCl_4-induced chronic liver injuries by increasing GP73 (Golgi protein-73)-mediated hepatic endoplasmic reticulum stress, while its overexpression alleviated liver injuries in male mice.[21] However, Wang et al[15] discovered that mice lacking ASGR1 fed a high-fat/high-cholesterol/bile salt diet for 4 to 6 weeks had grossly normal liver morphology. These findings indicate that the biological function of ASGR1 in the liver is worthy of discussion. In our study, the plasma AST level in female *Asgr1*$^{-/-}$*ApoE*$^{-/-}$ mice fed a WD significantly increased, and both female and male *Asgr1*$^{-/-}$*ApoE*$^{-/-}$ mice fed a WD showed significant worse morphology and more severe liver fibrosis (Figure 3); however, the plasma ALT level significantly decreased and liver injuries and liver fibrosis alleviated in total ASGR1-overexpressing mice (*ApoE*$^{-/-}$+AAV-ASGR1) fed a WD (Figure 6), thus supporting genetic susceptibility to liver injury in *Asgr1*$^{-/-}$ mice. What is more, the plasma ALT and AST levels in HFD-fed *Asgr1*$^{+/-}$ mice, the plasma AST level in HFD-fed *Asgr1*$^{-/-}$ mice, and sirius red staining results in HFD-fed *Asgr1*$^{-/-}$ mice were significantly increased compared with those in the *Asgr1*$^{+/+}$ group, indicating the ASGR1 deficiency in mice subjected to HFD causes liver injury (Figure S4A and S4D). However, there were no significant liver injury alterations both in ND-fed (Figure S5) and high-fat and high-cholesterol diet–fed (Figure S6) *Asgr1*$^{+/+}$, *Asgr1*$^{+/-}$, and *Asgr1*$^{-/-}$ mice. In addition, oral glucose tolerance test and insulin tolerance test assay results showed that only the oral glucose tolerance test was impaired in *Asgr1*$^{-/-}$ mice fed an HFD (Figure S15) compared with *Asgr1*$^{+/+}$ mice; meanwhile, there were no significant changes on the effects of oral glucose tolerance test and insulin tolerance test in *Asgr1*$^{-/-}$ mice fed an ND (Figure S16) and a high-fat and high-cholesterol diet (Figure S17) compared with *Asgr1*$^{+/+}$ mice. Taken together, ASGR1 deficiency exacerbated liver injury in WD-induced *Asgr1*$^{-/-}$*ApoE*$^{-/-}$ mice and HFD-induced *Asgr1*$^{-/-}$ mice, while its overexpression mitigated liver injury in WD-induced ASGR1-overexpressing *ApoE*$^{-/-}$ mice.

Moreover, we speculate that the reasons why ASGR1 total deficiency in *ApoE*$^{-/-}$ mice causes liver injury and lipid accumulation might be related to the downregulating effect on ACC phosphorylation and the upregulating effect on LXRα expression (Figure 8B). *ACC* is a key regulatory gene for lipid synthesis. The energy sensor AMPK plays an important role in regulating fatty acid synthesis through phosphorylation and inactivation of ACC.[42] Though ASGR1 deficiency activates the AMPK signaling pathway, it increases the downstream ACC and decreases its phosphorylation (Figure 8B), which might increase lipid synthesis in the liver; this effect of ASGR1 on ACC was also confirmed in ASGR1-overexpressing mice (Figure 8C). In addition, ASGR1 deficiency in *Asgr1*$^{-/-}$*ApoE*$^{-/-}$ mice increased the protein levels of LXRα (Figure 8B). LXRα activation can increase the expression of ABCA1, which is involved in maintaining cholesterol and lipid homeostasis and is beneficial for inhibiting atherosclerosis. However, LXRα activation also increases the expression of SREBP-1c, which is the master regulator of fatty acid synthesis.[54] Therefore, the effects of ASGR1 on liver injury and lipid accumulation are the combined results of the alterations in many lipid synthesis and metabolism-related genes.

In summary, our study reveals a crucial role of ASGR1 in the regulation of atherosclerotic plaque development and progression in the classic *ApoE*$^{-/-}$ mouse model of atherosclerosis. Mechanistically, ASGR1 regulates lipoprotein VLDL and LDL metabolism and cholesterol efflux by regulating the expression or activity of key proteins in VLDL synthesis, TG hydrolysis, LDL uptake, and cholesterol efflux. Our study provides a new and broader understanding of ASGR1 in the regulation of atherosclerosis and strong evidence for ASGR1 to be developed as a drug target for the treatment of atherosclerosis, but its effect on liver injury should be noted.

ARTICLE INFORMATION

Received April 9, 2024; accepted September 23, 2024.

Affiliations

State Key Laboratory of Bioactive Substance and Function of Natural Medicines, NHC (National Health Commission) Key Laboratory of Biotechnology of Antibiotics, National Center for New Microbial Drug Screening, Institute of Medicinal Biotechnology, Chinese Academy of Medical Sciences & Peking Union Medical College, Beijing, China (Yuyan Zhang, X.J., W.W., L.L., R.S., S.L., J.L., J.Z., X.H., Y.L., Yuhao Zhang, C.W., S.S., Y.X.). Department of Medicine, Aab Cardiovascular Research Institute, University of Rochester School of Medicine and Dentistry, NY (J.L., H.L., Z.-G.J.).

Acknowledgments

The authors thank LetPub (www.letpub.com) for its linguistic assistance during the preparation of this article.

Sources of Funding

This work was supported by grants from CAMS (Chinese Academy of Medical Sciences) Innovation Fund for Medical Sciences (2021-I2M-1-030), CAMS Fundamental Research Funds (2022-JKCS-10), the National Natural Science Foundation of China (82404723 and 81573482), and US NIH grants (HL141171 and HL130167 to Z.G.J.).

Disclosures

None.

Supplemental Material

Supplemental Materials & Methods
Tables S1 and S2
Figures S1–S18
Major Resources Table

REFERENCES

1. Gaudet D, Drouin-Chartier JP, Couture P. Lipid metabolism and emerging targets for lipid-lowering therapy. *Can J Cardiol*. 2017;33:872–882. doi: 10.1016/j.cjca.2016.12.019
2. Libby P, Buring JE, Badimon L, Hansson GK, Deanfield J, Bittencourt MS, Tokgozoglu L, Lewis EF. Atherosclerosis. *Nat Rev Dis Primers*. 2019;5:56. doi: 10.1038/s41572-019-0106-z
3. Libby P. The changing landscape of atherosclerosis. *Nature*. 2021;592:524–533. doi: 10.1038/s41586-021-03392-8
4. Shapiro MD, Fazio S. From lipids to inflammation: new approaches to reducing atherosclerotic risk. *Circ Res*. 2016;118:732–749. doi: 10.1161/CIRCRESAHA.115.306471
5. Luo J, Wang JK, Song BL. Lowering low-density lipoprotein cholesterol: from mechanisms to therapies. *Life Metab*. 2022;1:25–38. doi: 10.1093/lifemeta/loac004
6. Hassan M, Wagdy K. ASGR1 - a new target for lowering non-HDL cholesterol. *Glob Cardiol Sci Pract*. 2016;2016:e201614. doi: 10.21542/gcsp.2016.14

7. Levin MG. Remnant lipoproteins as a target for atherosclerosis risk reduction. *Arterioscler Thromb Vasc Biol*. 2021;41:2076–2079. doi: 10.1161/ATVBAHA.121.316341
8. Nioi P, Sigurdsson A, Thorleifsson G, Helgason H, Agustsdottir AB, Norddahl GL, Helgadottir A, Magnusdottir A, Jonasdottir A, Gretarsdottir S, et al. Variant ASGR1 associated with a reduced risk of coronary artery disease. *N Engl J Med*. 2016;374:2131–2141. doi: 10.1056/NEJMoa1508419
9. Ali L, Cupido AJ, Rijkers M, Hovingh GK, Holleboom AG, Dallinga-Thie GM, Stroes ESG, van den Boogert MAW. Common gene variants in ASGR1 gene locus associate with reduced cardiovascular risk in absence of pleiotropic effects. *Atherosclerosis*. 2020;306:15–21. doi: 10.1016/j.atherosclerosis.2020.07.001
10. Spiess M, Lodish HF. Sequence of a second human asialoglycoprotein receptor: conservation of two receptor genes during evolution. *Proc Natl Acad Sci USA*. 1985;82:6465–6469. doi: 10.1073/pnas.82.19.6465
11. Igdoura SA. Asialoglycoprotein receptors as important mediators of plasma lipids and atherosclerosis. *Curr Opin Lipidol*. 2017;28:209–212. doi: 10.1097/MOL.0000000000000395
12. Harris RL, van den Berg CW, Bowen DJ. ASGR1 and ASGR2, the genes that encode the asialoglycoprotein receptor (Ashwell receptor), are expressed in peripheral blood monocytes and show interindividual differences in transcript profile. *Mol Biol Int*. 2012;2012:283974. doi: 10.1155/2012/283974
13. Hrzenjak A, Frank S, Wo X, Zhou Y, Van Berkel T, Kostner GM. Galactose-specific asialoglycoprotein receptor is involved in lipoprotein (a) catabolism. *Biochem J*. 2003;376:765–771. doi: 10.1042/BJ20030932
14. Xu Y, Tao J, Yu X, Wu Y, Chen Y, You K, Zhang J, Getachew A, Pan T, Zhuang Y, et al. Hypomorphic ASGR1 modulates lipid homeostasis via INSIG1-mediated SREBP signaling suppression. *JCI Insight*. 2021;6:e147038. doi: 10.1172/jci.insight.147038
15. Wang JQ, Li LL, Hu A, Deng G, Wei J, Li YF, Liu YB, Lu XY, Qiu ZP, Shi XJ, et al. Inhibition of ASGR1 decreases lipid levels by promoting cholesterol excretion. *Nature*. 2022;608:413–420. doi: 10.1038/s41586-022-05006-3
16. Kingwell K. Inhibiting ASGR1 boosts cholesterol removal. *Nat Rev Drug Discov*. 2022;21:712. doi: 10.1038/d41573-022-00153-8
17. Huynh K. ASGR1 inhibition stimulates cholesterol excretion. *Nat Rev Cardiol*. 2022;19:642. doi: 10.1038/s41569-022-00768-9
18. Rader DJ. Targeting ASGR1 to lower cholesterol. *Nat Metab*. 2022;4:967–969. doi: 10.1038/s42255-022-00623-8
19. Xie B, Shi X, Li Y, Xia B, Zhou J, Du M, Xing X, Bai L, Liu E, Alvarez F, et al. Deficiency of ASGR1 in pigs recapitulates reduced risk factor for cardiovascular disease in humans. *PLoS Genet*. 2021;17:e1009891. doi: 10.1371/journal.pgen.1009891
20. Shi R, Wang J, Zhang Z, Leng Y, Chen AF. ASGR1 promotes liver injury in sepsis by modulating monocyte-to-macrophage differentiation via NF-kappaB/ATF5 pathway. *Life Sci*. 2023;315:121339. doi: 10.1016/j.lfs.2022.121339
21. Zhang Z, Leng XK, Zhai YY, Zhang X, Sun ZW, Xiao JY, Lu JF, Liu K, Xia B, Gao Q, et al. Deficiency of ASGR1 promotes liver injury by increasing GP73-mediated hepatic endoplasmic reticulum stress. *Nat Commun*. 2024;15:1908. doi: 10.1038/s41467-024-46135-9
22. Zhao W, Xu S, Weng J. ASGR1: an emerging therapeutic target in hypercholesterolemia. *Signal Transduct Target Ther*. 2023;8:43. doi: 10.1038/s41392-023-01319-5
23. Xu Y, Liu C, Han X, Jia X, Li Y, Liu C, Li N, Liu L, Liu P, Jiang X, et al. E17241 as a novel ABCA1 (ATP-binding cassette transporter A1) upregulator ameliorates atherosclerosis in mice. *Arterioscler Thromb Vasc Biol*. 2021;41:e284–e298. doi: 10.1161/ATVBAHA.120.314156
24. Kleiner DE, Brunt EM, Van Natta M, Behling C, Contos MJ, Cummings OW, Ferrell LD, Liu YC, Torbenson MS, Unalp-Arida A, et al; Nonalcoholic Steatohepatitis Clinical Research Network. Design and validation of a histological scoring system for nonalcoholic fatty liver disease. *Hepatology*. 2005;41:1313–1321. doi: 10.1002/hep.20701
25. Daugherty A, Tall AR, Daemen M, Falk E, Fisher EA, García-Cardeña G, Lusis AJ, Owens AP 3rd, Rosenfeld ME, Virmani R, et al. Recommendation on design, execution, and reporting of animal atherosclerosis studies: a scientific statement from the American Heart Association. *Arterioscler Thromb Vasc Biol*. 2017;37:e131–e157. doi: 10.1161/ATV.0000000000000062
26. Yang M, Liu Q, Huang T, Tan W, Qu L, Chen T, Pan H, Chen L, Liu J, Wong CW, et al. Dysfunction of estrogen-related receptor alpha-dependent hepatic VLDL secretion contributes to sex disparity in NAFLD/NASH development. *Theranostics*. 2020;10:10874–10891. doi: 10.7150/thno.47037
27. Lu Y, Cui X, Zhang L, Wang X, Xu Y, Qin Z, Liu G, Wang Q, Tian K, Lim KS, et al. The functional role of lipoproteins in atherosclerosis: novel directions for diagnosis and targeting therapy. *Aging Dis*. 2022;13:491–520. doi: 10.14336/AD.2021.0929
28. Yue JT, Abraham MA, LaPierre MP, Mighiu PI, Light PE, Filippi BM, Lam TK. A fatty acid-dependent hypothalamic-DVC neurocircuitry that regulates hepatic secretion of triglyceride-rich lipoproteins. *Nat Commun*. 2015;6:5970. doi: 10.1038/ncomms6970
29. Chen Z, Newberry EP, Norris JY, Xie Y, Luo J, Kennedy SM, Davidson NO. ApoB100 is required for increased VLDL-triglyceride secretion by microsomal triglyceride transfer protein in OB/OB mice. *J Lipid Res*. 2008;49:2013–2022. doi: 10.1194/jlr.M800240-JLR200
30. Wu SA, Kersten S, Qi L. Lipoprotein lipase and its regulators: an unfolding story. *Trends Endocrinol Metab*. 2021;32:48–61. doi: 10.1016/j.tem.2020.11.005
31. Basu D, Goldberg IJ. Regulation of lipoprotein lipase-mediated lipolysis of triglycerides. *Curr Opin Lipidol*. 2020;31:154–160. doi: 10.1097/MOL.0000000000000676
32. Groenen AG, Halmos B, Tall AR, Westerterp M. Cholesterol efflux pathways, inflammation, and atherosclerosis. *Crit Rev Biochem Mol Biol*. 2021;56:426–439. doi: 10.1080/10409238.2021.1925217
33. Chen L, Zhao ZW, Zeng PH, Zhou YJ, Yin WJ. Molecular mechanisms for ABCA1-mediated cholesterol efflux. *Cell Cycle*. 2022;21:1121–1139. doi: 10.1080/15384101.2022.2042777
34. Wang HH, Liu M, Portincasa P, Wang DQ. Recent advances in the critical role of the sterol efflux transporters ABCG5/G8 in health and disease. *Adv Exp Med Biol*. 2020;1276:105–136. doi: 10.1007/978-981-15-6082-8_8
35. Zhang Y, Breevoort SR, Angdisen J, Fu M, Schmidt DR, Holmstrom SR, Kliewer SA, Mangelsdorf DJ, Schulman IG. Liver LXRalpha expression is crucial for whole body cholesterol homeostasis and reverse cholesterol transport in mice. *J Clin Invest*. 2012;122:1688–1699. doi: 10.1172/JCI59817
36. Bao LD, Li CQ, Peng R, Ren XH, Ma RL, Wang Y, Lv HJ. Correlation between the decrease of cholesterol efflux from macrophages in patients with type II diabetes mellitus and down-regulated CYP7A1 expression. *Genet Mol Res*. 2015;14:8716–8724. doi: 10.4238/2015.July.31.20
37. Xu X, Zhang A, Halquist MS, Yuan X, Henderson SC, Dewey WL, Li PL, Li N, Zhang F. Simvastatin promotes NPC1-mediated free cholesterol efflux from lysosomes through CYP7A1/LXRα signalling pathway in oxLDL-loaded macrophages. *J Cell Mol Med*. 2017;21:364–374. doi: 10.1111/jcmm.12970
38. Zhu R, Ou Z, Ruan X, Gong J. Role of liver X receptors in cholesterol efflux and inflammatory signaling (review). *Mol Med Rep*. 2012;5:895–900. doi: 10.3892/mmr.2012.758
39. Azzu V, Vacca M, Kamzolas I, Hall Z, Leslie J, Carobbio S, Virtue S, Davies SE, Lukasik A, Dale M, et al. Suppression of insulin-induced gene 1 (INSIG1) function promotes hepatic lipid remodelling and restrains NASH progression. *Mol Metab*. 2021;48:101210. doi: 10.1016/j.molmet.2021.101210
40. Wu S, Zou MH. AMPK, mitochondrial function, and cardiovascular disease. *Int J Mol Sci*. 2020;21:4987. doi: 10.3390/ijms21144987
41. Gao L, Xu Z, Huang Z, Tang Y, Yang D, Huang J, He L, Liu M, Chen Z, Teng Y. CPI-613 rewires lipid metabolism to enhance pancreatic cancer apoptosis via the AMPK-ACC signaling. *J Exp Clin Cancer Res*. 2020;39:73. doi: 10.1186/s13046-020-01579-x
42. Steinberg GR, Carling D. AMP-activated protein kinase: the current landscape for drug development. *Nat Rev Drug Discov*. 2019;18:527–551. doi: 10.1038/s41573-019-0019-2
43. Sandesara PB, Virani SS, Fazio S, Shapiro MD. The forgotten lipids: triglycerides, remnant cholesterol, and atherosclerotic cardiovascular disease risk. *Endocr Rev*. 2019;40:537–557. doi: 10.1210/er.2018-00184
44. Huang JK, Lee HC. Emerging evidence of pathological roles of very-low-density lipoprotein (VLDL). *Int J Mol Sci*. 2022;23:4300. doi: 10.3390/ijms23084300
45. Gibbons GF. Assembly and secretion of hepatic very-low-density lipoprotein. *Biochem J*. 1990;268:1–13. doi: 10.1042/bj2680001
46. Whitacre BE, Howles P, Street S, Morris J, Swertfeger D, Davidson WS. Apolipoprotein E content of VLDL limits LPL-mediated triglyceride hydrolysis. *J Lipid Res*. 2022;63:100157. doi: 10.1016/j.jlr.2021.100157
47. Ohashi R, Mu H, Wang X, Yao Q, Chen C. Reverse cholesterol transport and cholesterol efflux in atherosclerosis. *QJM*. 2005;98:845–856. doi: 10.1093/qjmed/hci136
48. Musso G, Gambino R, Cassader M. Cholesterol metabolism and the pathogenesis of non-alcoholic steatohepatitis. *Prog Lipid Res*. 2013;52:175–191. doi: 10.1016/j.plipres.2012.11.002
49. Wang B, Tontonoz P. Liver X receptors in lipid signalling and membrane homeostasis. *Nat Rev Endocrinol*. 2018;14:452–463. doi: 10.1038/s41574-018-0037-x

50. Guan B, Tong J, Hao H, Yang Z, Chen K, Xu H, Wang A. Bile acid coordinates microbiota homeostasis and systemic immunometabolism in cardiometabolic diseases. *Acta Pharm Sin B*. 2022;12:2129–2149. doi: 10.1016/j.apsb.2021.12.011
51. Uppal H, Saini SP, Moschetta A, Mu Y, Zhou J, Gong H, Zhai Y, Ren S, Michalopoulos GK, Mangelsdorf DJ, et al. Activation of LXRs prevents bile acid toxicity and cholestasis in female mice. *Hepatology*. 2007;45:422–432. doi: 10.1002/hep.21494
52. Zhu X, Song G, Zhang S, Chen J, Hu X, Zhu H, Jia X, Li Z, Song W, Chen J, et al. Asialoglycoprotein receptor 1 functions as a tumor suppressor in liver cancer via inhibition of STAT3. *Cancer Res*. 2022;82:3987–4000. doi: 10.1158/0008-5472.CAN-21-4337
53. Svecla M, Da Dalt L, Moregola A, Nour J, Baragetti A, Uboldi P, Donetti E, Arnaboldi L, Beretta G, Bonacina F, et al. ASGR1 deficiency diverts lipids toward adipose tissue but results in liver damage during obesity. *Cardiovasc Diabetol*. 2024;23:42. doi: 10.1186/s12933-023-02099-6
54. Savla SR, Prabhavalkar KS, Bhatt LK. Liver X receptor: a potential target in the treatment of atherosclerosis. *Expert Opin Ther Targets*. 2022;26:645–658. doi: 10.1080/14728222.2022.2117610